NACA RM No. L8L29

NACA

RESEARCH MEMORANDUM

LOW-SPEED STATIC-STABILITY AND ROLLING CHARACTERISTICS OF LOW-ASPECT-RATIO WINGS OF TRIANGULAR AND MODIFIED TRIANGULAR PLAN FORMS

By

Byron M. Jaquet and Jack D. Brewer

Langley Aeronautical Laboratory
Langley Air Force Base, Va.

NATIONAL ADVISORY COMMITTEE
FOR AERONAUTICS

WASHINGTON

March 29, 1949
Declassified December 14, 1953

NATIONAL ADVISORY COMMITTEE FOR AERONAUTICS

RESEARCH MEMORANDUM

LOW-SPEED STATIC-STABILITY AND ROLLING CHARACTERISTICS OF LOW-ASPECT-RATIO WINGS OF TRIANGULAR AND MODIFIED TRIANGULAR PLAN FORMS

By Byron M. Jaquet and Jack D. Brewer

SUMMARY

A low-speed investigation was made in the Langley stability tunnel to determine experimentally the effects of changes in profile and aspect ratio on the low-speed static-stability and rolling characteristics of triangular wings. The investigation was extended to determine the effects of adding fins to the upper surface and of cutting portions from the tips of a triangular wing to form low-aspect-ratio tapered wings.

In general, profile had little effect on the static-stability and rolling characteristics of triangular wings at low lift coefficients. The greatest effect of profile was in the high-lift-coefficient range. The linear range of the static-stability parameters was decreased (in much the same manner as for untapered swept wings) as the leading-edge sharpness was increased.

Several of the characteristics of triangular wings may be estimated with fair accuracy by available swept-wing theory. Available low-aspect-ratio triangular-wing theory was found to be reliable for certain characteristics, but for others, particularly the lift-curve slope, aerodynamic center position, and the damping in roll, the agreement was poor except at the lowest test aspect ratio ($A = 1.07$).

The vertical fins tested provided good directional stability throughout the entire lift-coefficient range. The fins increased the damping in roll and decreased the variation of the effective dihedral parameter with lift coefficient.

The series of modified triangular wings obtained by cutting various portions from the tips of a basic triangular wing generally had good longitudinal and directional stability but very high effective dihedral. Most of the characteristics of these wings, at low lift coefficients, could be predicted with fair accuracy by available swept-wing theory.

INTRODUCTION

The advantages of low-aspect-ratio pointed wings for high-speed flight have been outlined by Jones in reference 1. Extensive theoretical investigations of the stability characteristics of triangular wings have been made in the supersonic speed range. Theoretical investigations in the subsonic speed range, however, are very limited. The theory of reference 2 is considered to be applicable only to thin triangular wings of aspect ratios less than 0.5 and the theory of references 3 and 4 presents only a few of the stability characteristics. The approximate theory of swept wings presented in reference 5 might be expected to be unreliable as the taper ratio decreases from unity.

The present investigation was conducted to determine experimentally the effects of changes in profile and aspect ratio on the low-speed static-stability and rolling characteristics of triangular wings. The investigation was extended to determine the effects of adding fins to the upper surface and of cutting portions from the tips of a triangular wing to form low-aspect-ratio tapered wings. Rolling characteristics were determined by means of the rolling-flow equipment of the Langley stability tunnel. (See reference 6.) The experimental data are compared with available theory.

SYMBOLS

The data presented herein are in the form of standard NACA coefficients of forces and moments which are referred to the stability system of axes with the origin at the projection of the quarter-chord point of the mean aerodynamic chord on the plane of symmetry. The positive directions of the forces, moments, and angular displacements are shown in figure 1. The symbols and coefficients used herein are defined as follows:

C_L lift coefficient (L/qS)

$C_{L_{max}}$ maximum lift coefficient

C_X longitudinal-force coefficient (X/qS)

C_Y lateral-force coefficient (Y/qS)

C_l rolling-moment coefficient (L'/qSb)

C_m pitching-moment coefficient ($M/qS\bar{c}$)

C_n yawing-moment coefficient (N/qSb)

L lift, pounds

X longitudinal force, pounds

Y lateral force, pounds

L' rolling moment about X-axis, foot-pounds

M pitching moment about Y-axis, foot-pounds

N yawing moment about Z-axis, foot-pounds

A aspect ratio $\left(\frac{b^2}{S}\right)$

b span, feet

S area, square feet

c local chord measured parallel to plane of symmetry, feet

$\bar{c}$ mean aerodynamic chord, feet $\left(\frac{2}{S}\int_0^{b/2} c^2\,dy\right)$

c_r root chord, feet

λ taper ratio

x longitudinal distance from apex of triangle to quarter-chord point of any chordwise section, feet

$\bar{x}$ longitudinal distance from apex of triangle to quarter-chord point of mean aerodynamic chord, feet $\left(\frac{2}{S}\int_0^{b/2} cx\,dy\right)$

R Reynolds number

ρ density of air, slugs per cubic foot

V free-stream velocity, feet per second

q dynamic pressure, pounds per square foot $\left(\frac{\rho V^2}{2}\right)$

α angle of attack in plane of symmetry, degrees

ψ angle of yaw, degrees

Λ_{LE} angle of sweepback of leading edge, degrees

$\Lambda_{c/4}$ angle of sweepback of quarter-chord line, degrees $\left(\cot^{-1}\frac{A}{3}\text{ for triangular wings}\right)$

$\frac{pb}{2V}$ helix angle generated by wing tip in roll, radians

p angular velocity in roll, radians per second

$$C_{L_\alpha} = \frac{\partial C_L}{\partial \alpha}$$

$$C_{l_\psi} = \frac{\partial C_l}{\partial \psi}$$

$$C_{n_\psi} = \frac{\partial C_n}{\partial \psi}$$

$$C_{Y_\psi} = \frac{\partial C_Y}{\partial \psi}$$

$$C_{l_p} = \frac{\partial C_l}{\partial \frac{pb}{2V}}$$

$$C_{n_p} = \frac{\partial C_n}{\partial \frac{pb}{2V}}$$

$$C_{Y_p} = \frac{\partial C_Y}{\partial \frac{pb}{2V}}$$

APPARATUS, MODELS, AND TEST

The present investigation was conducted in the 6-foot-diameter rolling-flow test section of the Langley stability tunnel which is described in detail in reference 6.

The relevant dimensions of the models and the test conditions are presented in table I; hereinafter, each model will be referred to by the number designated in the table. All profiles referred to are parallel to the plane of symmetry.

All the tests were made on a six-component strain-gage balance strut with the models mounted at a point two-thirds of the root chord from the apex of the triangles.

Figure 2 presents the profiles of the series of models having 60° sweepback of the leading edge (models 1, 2, and 3). The models were constructed of laminated mahogany and were given highly polished surfaces. Flat-plate fins of aspect ratio 0.77 and 1.15 were constructed of laminated mahogany and were tested on model 2. Various portions of the tips of the triangular wing of aspect ratio 4 (model 7) were cut off (parallel to the plane of symmetry) to give aspect ratios 3 (model 8), 2 (model 9), and 1 (model 10), including tips of revolution.

All the models were tested with a small canopy covering the strut head and the cut-out to prevent leakage of air through the wing.

Photographs of some of the models are presented in figures 3 to 7.

Three series of tests were made. In the first series the lift, longitudinal force, and pitching moment were measured at $\psi = 0°$ through an angle-of-attack range from about $\alpha = -4°$ to an angle of attack beyond the stall. In the second series of tests the static derivatives were determined by measuring the lateral force, rolling moment, and yawing moment at $\psi = \pm 5°$ through the same angle-of-attack range. In the third series the models were tested through the angle-of-attack range at the values of $pb/2V$ listed in table I to obtain the rolling derivatives C_{l_p}, C_{n_p}, and C_{Y_p}.

All the tests were made at a dynamic pressure of 24.9 pounds per square foot which, when based on the mean aerodynamic chords of the models, corresponds to the Reynolds numbers in table I. The test Mach number was 0.13.

CORRECTIONS AND ACCURACY

The test data were transferred from the model-mounting position (a point at two-thirds of the root chord from the apex of the triangles) to the quarter-chord point of the mean aerodynamic chord.

The angle of attack, longitudinal-force coefficient, and rolling-moment coefficient were corrected for jet boundary effects, but corrections were not applied to account for model blocking, which amounts to an error of about 1.5 percent in dynamic pressure.

In the rolling-flow tests, tares appeared to be negligible up to approximately $\alpha = 16^{\circ}$. However, at high angles of attack, there appeared to be large support interference, and since these effects could not be accurately evaluated, the rolling derivatives are not presented for angles of attack greater than approximately 16°.

The measurements taken are believed to be accurate within the following amounts which are based on the maximum values of the forces and moments for model 6:

α, deg	± 0.1
ψ, deg	± 0.2
C_L	± 0.0029
C_X	± 0.0045
C_m	± 0.0045
C_l	± 0.0004
C_n	± 0.0003
C_Y	± 0.0046

RESULTS AND DISCUSSION

Presentation of Results

The static and rolling characteristics of the models of the present investigation are presented in the four groups of basic data and the two summary groups shown in the following table:

	Figure
Effect of profile of triangular wings	8, 9, 10
Effect of aspect ratio of triangular wings	11, 12, 13
Effect of vertical fins	14, 15, 16
Effect of aspect ratio of modified triangular wings	17, 18, 19
Summary effects of aspect ratio of triangular wings	20, 21, 22
Summary effects of aspect ratio of modified triangular wings	23, 24, 25

All theoretical values obtained from reference 5 have been calculated by use of the equations and have been extrapolated to the appropriate taper ratios.

Effect of Profile of Triangular Wings

Changes in wing profile appear to have rather large effects on the lift, longitudinal-force, and pitching-moment characteristics at moderate and high lift coefficients as is indicated in figure 8. The highest maximum lift coefficient was obtained with the flat-plate wing (model 1) and the lowest with the biconvex (12-percent-thick) wing (model 3). The NACA 0012 wing (model 2) gave gradually increasing longitudinal stability throughout the lift-coefficient range. Reductions in longitudinal stability were obtained at $C_L = 0.4$ for both the flat-plate wing and the biconvex wing. (See fig. 8.) For all three models the directional stability increased with lift coefficient up to $C_L = 0.9$, after which the directional stability decreased to about zero at maximum lift coefficient. (See fig. 9.)

Certain characteristics appear to have a consistent relation to the shape of the airfoil leading edge. The effective dihedral parameter C_{l_ψ}, for example, varies almost linearly up to $C_L = 0.4$ for the blunt-nose NACA 0012 airfoil. For the sharper nose flat-plate and biconvex airfoils C_{l_ψ} is linear only to a lift coefficient of 0.25. The decrease in the initial linear range of the effective dihedral parameter as the leading edge was effectively sharpened was noted in tests of untapered swept wing in reference 7. Similar trends are noted, but to a lesser degree, for the lift-curve slope (fig. 8) and for the variations on the rolling derivatives C_{Y_p} and C_{n_p} with lift coefficient (fig. 10). Negative values of C_{n_p} (as predicted by the theories of references 2 and 5) were obtained only for the NACA 0012 profile model and then only to a lift coefficient of 0.5. No consistent effects of airfoil section are noted for the damping in roll over the range of lift coefficients for which the data are presented.

Effect of Aspect Ratio of Triangular Plan Forms

It should be remembered that in the following discussion of the effect of aspect ratio of triangular plan forms there are also effects of sweep present, since the sweep angle is automatically increased as the aspect ratio is decreased.

As the aspect ratio is reduced, C_{L_α} is decreased (at low lift coefficients) and $C_{L_{max}}$ occurs at higher angles of attack. This trend was noted in reference 8 in tests of similar triangular-wing models. At $C_L = 0.3$ a sharp increase in C_{L_α} occurs for model 4; increased longitudinal stability is noted at the same lift coefficient. An opposite trend is noted for model 7 at $C_L = 0.6$ where a decrease occurs in the

longitudinal stability and in the lift-curve slope. Increased longitudinal stability is noted throughout the lift-coefficient range as the aspect ratio is decreased. (See fig. 11.) As the aspect ratio is reduced the aerodynamic center moves rearward toward the 50-percent-chord point (fig. 20) as is indicated for very low aspect ratios by the theory of reference 2. The theory of reference 3 indicates a more gradual movement of the aerodynamic center starting from a more forward position. It should be noted that reference 3 neglects any possible changes in the chordwise pressure distributions of the wing. The empirical curve taken from reference 8 indicates the same trend as the experimental; however, the aerodynamic center is in a more forward position than the results of the present investigation indicate. It should be noted that all the triangular wings tested in reference 8 had flat-plate airfoil sections, whereas those tested herein had an NACA 0012 profile with a larger trailing-edge angle and a blunt leading edge. Large-scale tests of a triangular wing with a double-wedge airfoil (5 percent thick at 20 percent chord) indicate about the same position of the aerodynamic center as does the present investigation for an aspect ratio of 2.0. (See reference 9.)

The trend of $C_{L_{max}}$ in figure 20 agrees with the trends of reference 8 in that the peak value of $C_{L_{max}}$ was reached at about the same aspect ratio. As the aspect ratio is decreased, the lift-curve slope is decreased as can be seen in figure 20. The swept-wing theory of references 3 and 5 shows fair agreement with the experimental data for the aspect-ratio range considered. The theory of reference 2 approaches the experimental values only as the aspect ratio approaches zero as would be expected.

It should be remembered that all the profiles for the models for which the data are presented in figure 12 are of NACA 0012 sections parallel to the plane of symmetry. With a highly swept model (as model 4) there is a very large area in the plane of symmetry forward of the quarter chord of the mean aerodynamic chord which, when the model is yawed or rolled, acts in the manner of a fin. Model 4, because of this area, has positive values of the directional-stability parameter C_{n_ψ} below $C_L = 0.73$. The model does have increasing directional stability at the stall while models 2 and 7 do not. If model 4 was equipped with a high-aspect-ratio fin, the objectionable characteristics below $C_L = 0.73$ might be overcome, resulting in a model having better over-all characteristics than models 2 or 7. The values of $\partial C_{n_\psi} / \partial C_L^2$ presented in figure 21 (obtained by plotting C_{n_ψ} against C_L^2 and taking slopes at $C_L = 0$) indicate increasing directional stability as the aspect ratio is decreased. (The values are not presented for model 4 because of the erratic nature of the curve of C_{n_ψ}.) The theory of reference 5 is in qualitative agreement with the experimental results. Very high maximum values of the

effective dihedral parameter C_{l_ψ} are obtained as the aspect ratio is decreased. (See fig. 12.) The rate of change of C_{l_ψ} with C_L increases as the aspect ratio decreases. (See fig. 21.) Although the values obtained from the theories of references 2 and 5 predict the trends, they are low in magnitude.

The slopes of the curves of C_{Y_p} in figure 13 were taken at $C_L = 0$ and are presented in figure 22. The curve from the theory of reference 2 shows good agreement with experiment down to an aspect ratio of 2.31 after which the experimental curve falls to zero at $A = 1.07$. The curve from the theory of reference 5 (derived for untapered swept wings) gives consistently high values of $\partial C_{Y_p}/\partial C_L$. The theories of references 2 and 5 predict negative values of C_{n_p} at positive lift coefficients; however, the experimental values of C_{n_p} are negative only at moderate lift coefficients. (See fig. 13.) The available theory is, therefore, extremely limited in the range of applicability to triangular plan forms. As the aspect ratio is decreased, $\partial C_{n_p}/\partial C_L$ at $C_L = 0$ increases negatively and the theory of reference 5 predicts the results with fair accuracy. (See fig. 22.) The curve from the theory of reference 2 indicates the proper trend, but the correlation with experiment is good only at the lowest test aspect ratio $A = 1.07$.

The results of reference 8 for flat-plate triangles indicate positive values of C_{l_p} at moderate lift coefficients for aspect ratios below the range considered herein. The opposite trend is noted herein for model 4 ($A = 1.07$) which shows an increase in C_{l_p} starting at a lift coefficient of about 0.1. (See fig. 13.) This increase is believed to be caused by the sudden increase in C_{L_α} (fig. 11) and the vertical-fin effect at the wing nose resulting from the use of a blunt-nose airfoil section in combination with a large sweep angle. At high angles of attack the vertical displacement of the nose from the axis of rotation causes an increase in damping in roll. The values of C_{l_p} (taken at $C_L = 0$ from fig. 13) presented in figure 22 show an almost linear decrease in damping as the aspect ratio is reduced. The theory of reference 4 is in good agreement with the experimental curve. The theory of reference 5 predicts the trend of the experimental curve but the magnitude is about 15 percent too high. The theory of reference 2 shows fair agreement with experiment only at the lowest test aspect ratio ($A = 1.07$).

Effect of Vertical Fins

The effects of the fins on C_L, C_m, and C_X (fig. 14) are small as would be expected.

Although the increment in C_{n_ψ} (fig. 15) caused by the small (A = 0.77) and large (A = 1.15) fins decreases from $C_L = 0$ to $C_L = 1.0$, C_{n_ψ} for the wing-fin combinations increases throughout the entire lift range. The addition of either fin causes a positive increment of C_{l_ψ} at $C_L = 0$ which decreases as the lift coefficient increases. Consequently, the rate of change of C_{l_ψ} with C_L for the wing-fin combinations is smaller than for the wing alone. (See fig. 15.)

Addition of the large fin caused negative displacements of C_{Y_p} at $C_L = 0$; the addition of either fin caused an increase in the rate of change of C_{Y_p} with C_L. (See fig. 16.) An almost constant positive increment in C_{n_p} is the result of adding the large fin to model 2. (See fig. 16.) Both the large and small fins increased the damping in roll throughout the lift-coefficient range; the increase for the large fin amounts to about 30 percent of the damping in roll of the wing alone.

Effect of Aspect Ratio of Modified Triangular Plan Forms

The models of the present group were formed by cutting various portions from the tips of a basic triangular wing (model 7) parallel to the plane of symmetry to obtain aspect ratio 3 (model 8), aspect ratio 2 (model 9), and aspect ratio 1 (model 10), including tips of revolution.

For the lowest test aspect ratio (A = 1.0) a definite nonlinear variation of C_L with α is noted in figure 17 which agrees with the results of similar models tested in reference 8. Except for a short range ($C_L = 0.15$ to $C_L = 0.3$) the variation of C_m with C_L is nonlinear for model 10 (A = 1.0). Reducing the aspect ratio of modified triangular wings results in a forward movement of the aerodynamic center which can be estimated with fair accuracy for aspect ratios of 2.3 or less by the theory of reference 3. (See fig. 23.) An increase in $C_{L_{max}}$ is noted as the aspect ratio is decreased. A similar trend was noted for the same range of aspect ratios reported in reference 8. The theories of references 3 and 5 predict a decrease in lift-curve slope with a decrease in aspect ratio but are only in fair agreement with the experimental results. (See fig. 23.) The theory of reference 2 shows poor agreement with experiment even for an aspect ratio of 1.0.

High directional stability is indicated at high lift coefficients for low aspect ratios in figure 18. Also indicated in figure 18 are very high values of the effective dihedral parameter C_{l_ψ} for low aspect ratios. Reducing the aspect ratio by cutting portions from the tips parallel to the plane of symmetry results in an increase in directional stability which is in fair agreement with the theory of reference 5 down to an aspect ratio of 2. (See fig. 24.) At an aspect ratio of 1.0 the directional stability is considerably larger than that predicted by reference 5. The increase in the variation of C_{l_ψ} with C_L with decreasing aspect ratio is considerably larger than is indicated by either reference 2 or reference 5. As the aspect ratio is decreased, C_{l_p} at high lift coefficients, has a tendency to increase. (See fig. 19.) The experimental variation of C_{Y_p} with C_L (fig. 25) shows little change with aspect ratio; whereas the theory of reference 5 indicates a small reduction in this parameter with decreasing aspect ratio and the triangular wing theory of reference 2 indicates a large increase in $\partial C_{Y_p}/\partial C_L$ with decreasing aspect ratio. In general, better agreement was obtained with reference 5. The experimental curve of figure 25 indicates a decrease in the variation of C_{n_p} with C_L with decreasing aspect ratio which is in fair agreement with the theory of reference 5. Reducing the aspect ratio results in a decrease in damping in roll C_{l_p}. (See fig. 25.) Good agreement is indicated with experiment by the theory of reference 5 while the theory of reference 2 is in fair agreement with experiment only at the lowest test aspect ratio ($A = 1.0$). The theory of reference 4 is in fair agreement at low aspect ratios and excellent agreement at $A = 3$ and $A = 4$.

CONCLUSIONS

Tests conducted in the 6-foot-diameter rolling-flow test section of the Langley stability tunnel to determine the effects of a number of geometric variables on the low-speed static-stability and rolling characteristics of triangular wings indicate the following conclusions:

1. In general, variations in profile had small effects on the static and rolling characteristics of triangular wings at low lift coefficients. The greatest effect of profile was in the high-lift-coefficient range. The linear range of the static-stability parameters was decreased (in much the same manner as for untapered swept wings) as the leading-edge sharpness was increased.

2. Several of the characteristics of triangular wings may be estimated with fair accuracy by available swept-wing theory. Available low-aspect-ratio triangular-wing theory was found to be reliable for

certain characteristics but for others, particularly the lift-curve slope, damping in roll, and aerodynamic-center position, the agreement was poor except at the lowest test aspect ratio (A = 1.07).

3. The vertical fins tested provided good directional stability for the wing-fin combinations throughout the lift-coefficient range. The fins increased the damping in roll and decreased the variation of effective dihedral parameter with lift coefficient.

4. The series of wings obtained by cutting various portions from the tips of a basic triangular wing generally had good longitudinal and directional stability but very high effective dihedral. Most of the characteristics of these wings, at low lift coefficients, could be predicted with fair accuracy by means of available swept-wing theory.

Langley Aeronautical Laboratory
National Advisory Committee for Aeronautics
Langley Air Force Base, Va.

REFERENCES

1. Jones, Robert T.: Properties of Low-Aspect-Ratio Pointed Wings at Speeds below and above the Speed of Sound. NACA Rep. No. 835, 1946.

2. Ribner, Herbert S.: The Stability Derivatives of Low-Aspect-Ratio Triangular Wings at Subsonic and Supersonic Speeds. NACA TN No. 1423, 1947.

3. DeYoung, John: Theoretical Additional Span Loading Characteristics of Wings with Arbitrary Sweep, Aspect Ratio, and Taper Ratio. NACA TN No. 1491, 1947.

4. Bird, John D.: Some Theoretical Low-Speed Span Loading Characteristics of Swept Wings in Roll and Sideslip. NACA TN No. 1839, 1949.

5. Toll, Thomas A., and Queijo, M. J.: Approximate Relations and Charts for Low-Speed Stability Derivatives of Swept Wings. NACA TN No. 1581, 1948.

6. MacLachlan, Robert, and Letko, William: Correlation of Two Experimental Methods of Determining the Rolling Characteristics of Unswept Wings. NACA TN No. 1309, 1947.

7. Letko, William, and Jaquet, Byron M.: Effect of Airfoil Profile of Symmetrical Sections on the Low-Speed Static-Stability and Yawing Derivatives of 45° Sweptback Wing Models of Aspect Ratio 2.61. NACA RM No. L8H10, 1948.

8. Tosti, Louis P.: Low-Speed Static Stability and Damping-in-Roll Characteristics of Some Swept and Unswept Low-Aspect-Ratio Wings. NACA TN No. 1468, 1947.

9. Anderson, Adrien E.: An Investigation at Low Speed of a Large-Scale Triangular Wing of Aspect Ratio Two.- II. The Effect of Airfoil Section Modifications and the Determination of the Wake Downwash. NACA RM No. A7H28, 1947.

TABLE I.- PERTINENT MODEL DIMENSIONS AND TEST CONDITIONS

Model	Profile	Plan form	$\Lambda_{L.E.}$ (deg)	$\Lambda_{c/4}$ (deg)	Aspect ratio	Span (in.)	Root chord (in.)	M.A.C. (in.)	$\bar{x}$ (in.)	Area (sq in.)	R	$\frac{pb}{2V}$ (radians)	Taper ratio
1	Flat plate		60	52.2	2.31	36.07	31.23	20.82	15.62	564.0	1.603×10^6	± 0.025 $\pm .075$	0
2	NACA 0012		60	52.2	2.31	36.50	31.60	21.10	15.80	576.0	1.624	$\pm .025$ $\pm .075$	0
3	Biconvex 12 percent		60	52.2	2.31	36.50	31.60	21.10	15.80	576.0	1.624	$\pm .025$ $\pm .075$	0
4	NACA 0012		75	70.4	1.07	24.85	46.37	30.90	23.20	576.0	2.380	$\pm .017$ $\pm .051$	0
5	NACA 0012 and flat-plate fin		Wing, 60 Fin, 68.9	52.2	Wing, 2.31 Fin, 0.77	Wing, 36.5 Fin, 12.16	31.60	21.10	15.80	Wing, 576 Fin, 192	1.624	$\pm .025$ $\pm .075$	0
6	NACA 0012 and flat-plate fin		Wing, 60 Fin, 60	52.2	Wing, 2.31 Fin, 1.15	Wing, 36.5 Fin, 18.25	31.60	21.10	15.80	Wing, 576 Fin, 288	1.624	$\pm .025$ $\pm .075$	0
7	NACA 0012		45	36.9	4.0	48.00	24.00	16.00	12.00	576.0	1.232	$\pm .033$ $\pm .099$	0
8	NACA 0012		45	36.9	3.0	41.20	24.00	16.30	11.77	563.6	1.254	$\pm .028$ $\pm .084$	0.15
9	NACA 0012		45	36.9	2.0	31.80	24.00	17.10	10.95	507.8	1.335	$\pm .022$ $\pm .066$	0.36
10	NACA 0012		45	36.9	1.0	18.80	24.00	19.60	9.13	355.8	1.510	$\pm .013$ $\pm .039$	0.58

NACA

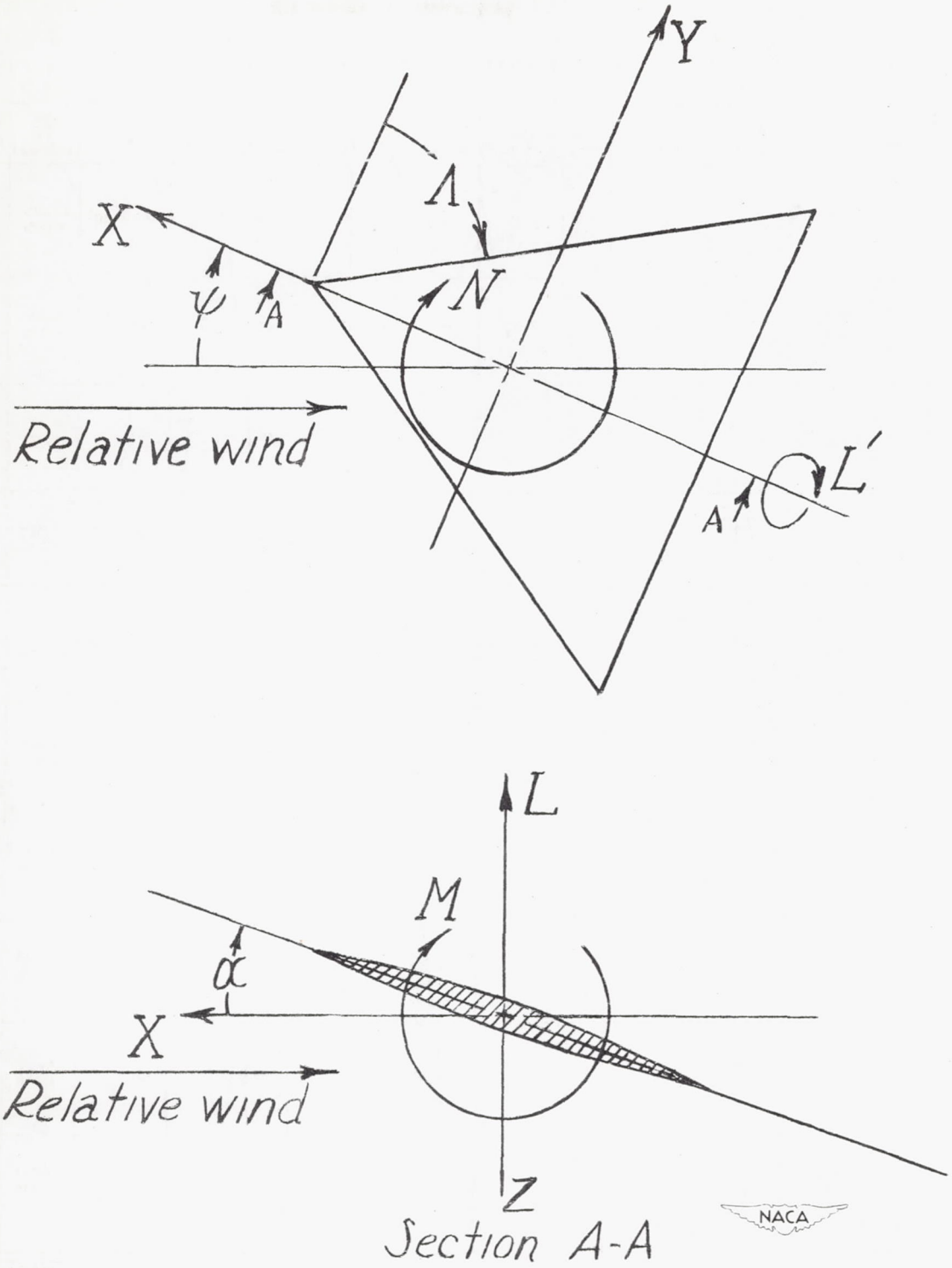

Figure 1.– System of stability axes. Positive forces, moments, and angles are indicated.

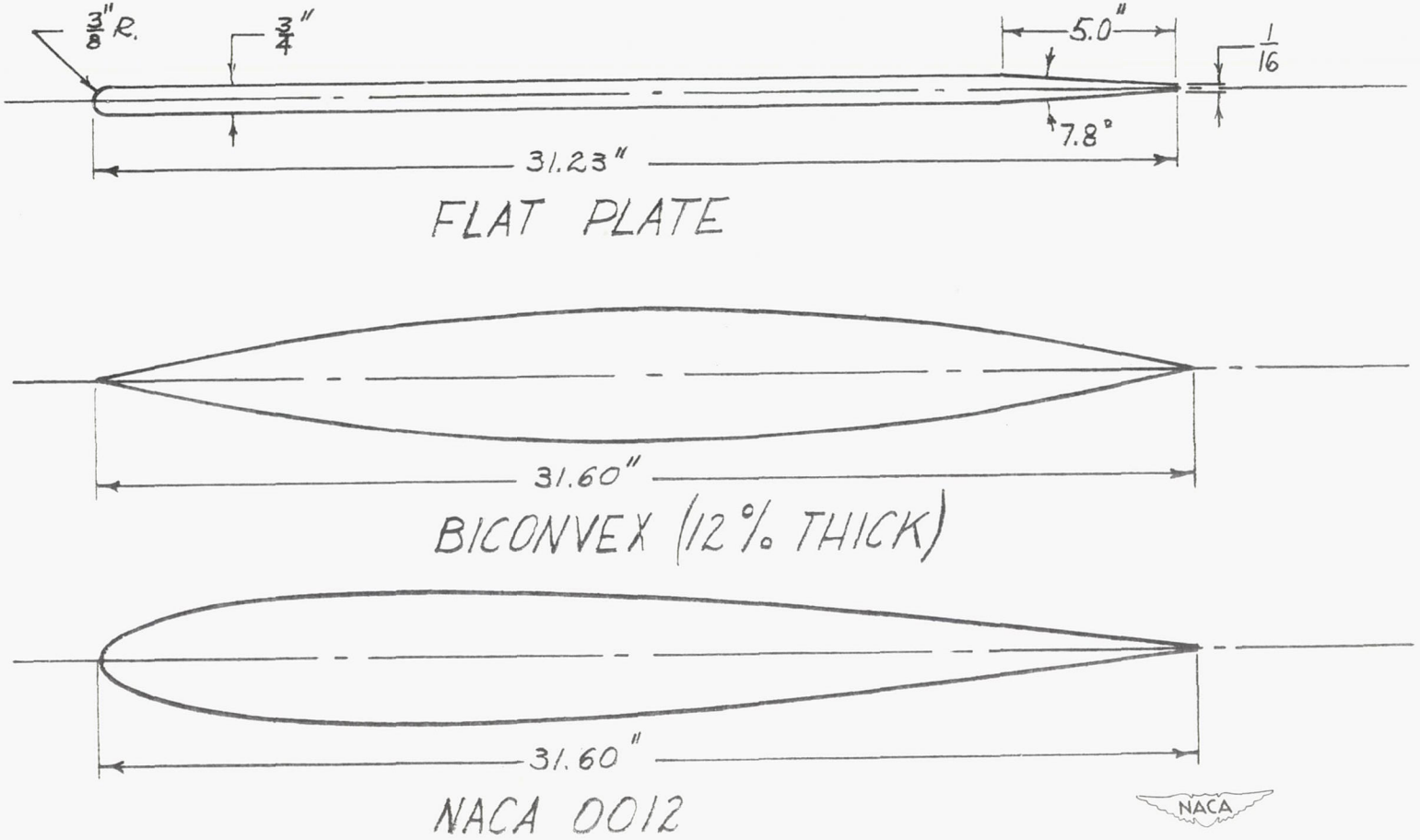

Figure 2.– Root–chord profiles of 60° triangular wings.

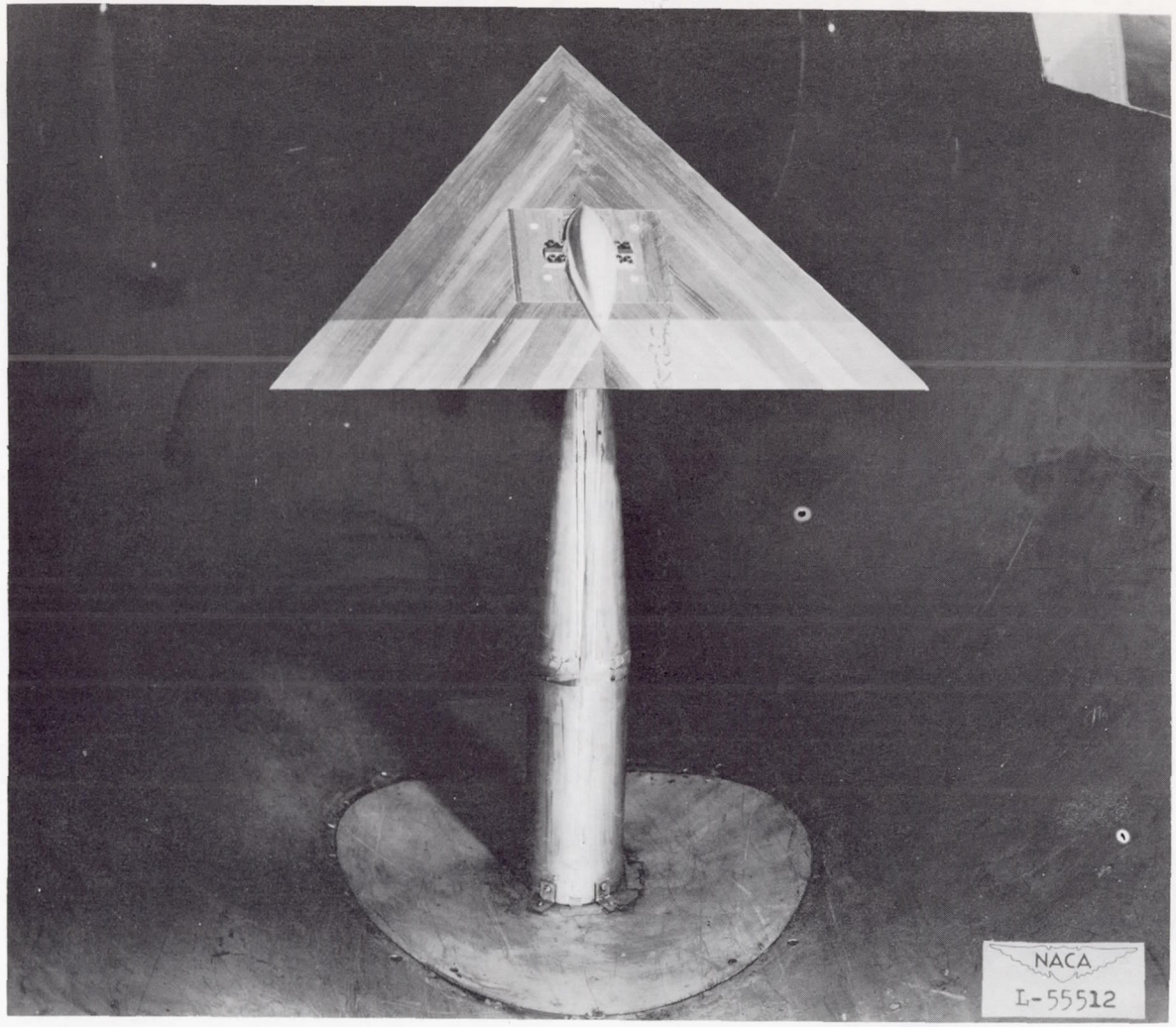

Figure 3.— Model 1 mounted in tunnel. A = 2.31; $\Lambda_{c/4}$ = 52.2°; profile, flat plate.

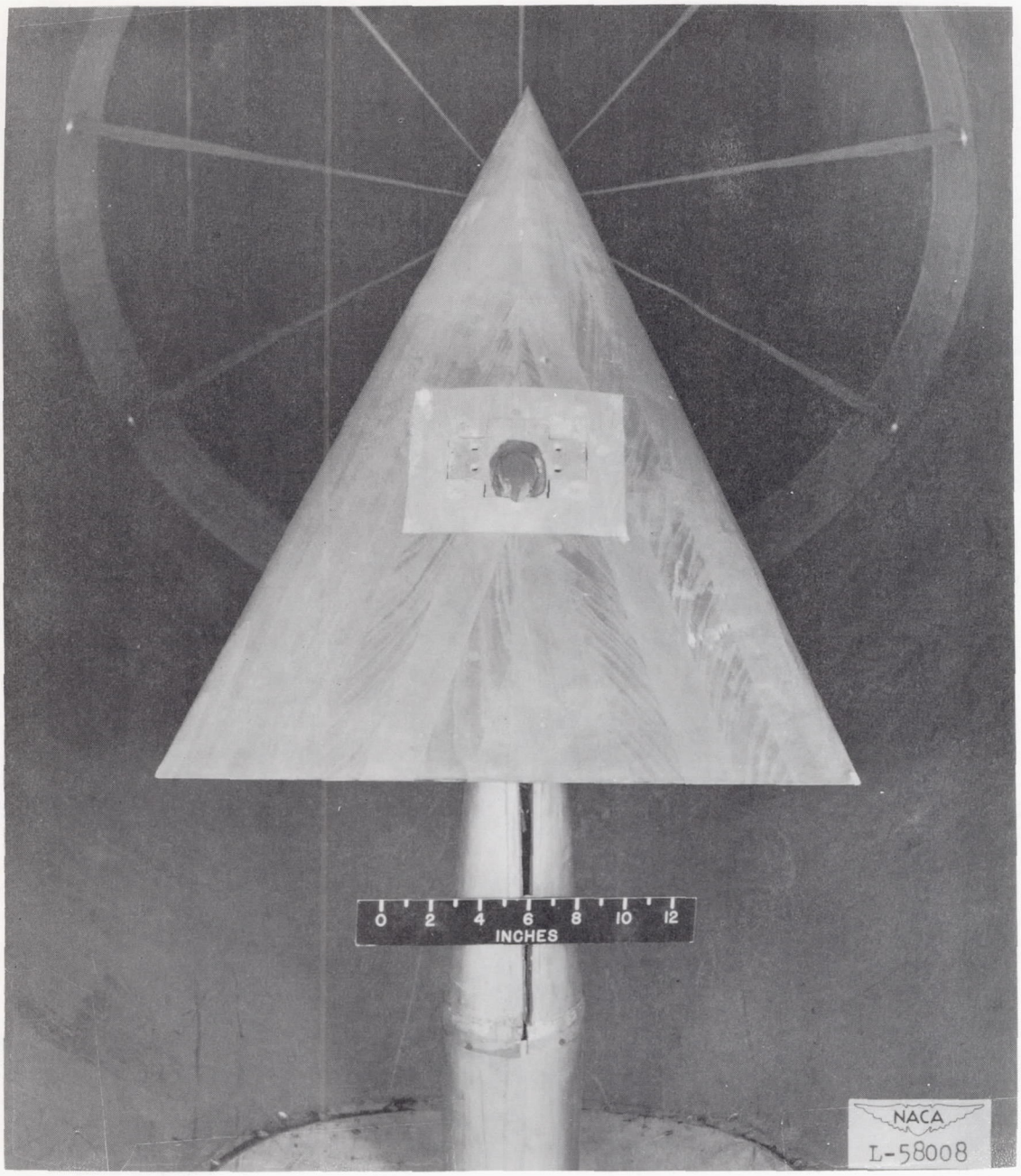

Figure 4.– Model 4 mounted in tunnel. A = 1.07; $\Lambda_{c/4} = 70.4^{\circ}$; profile, NACA 0012.

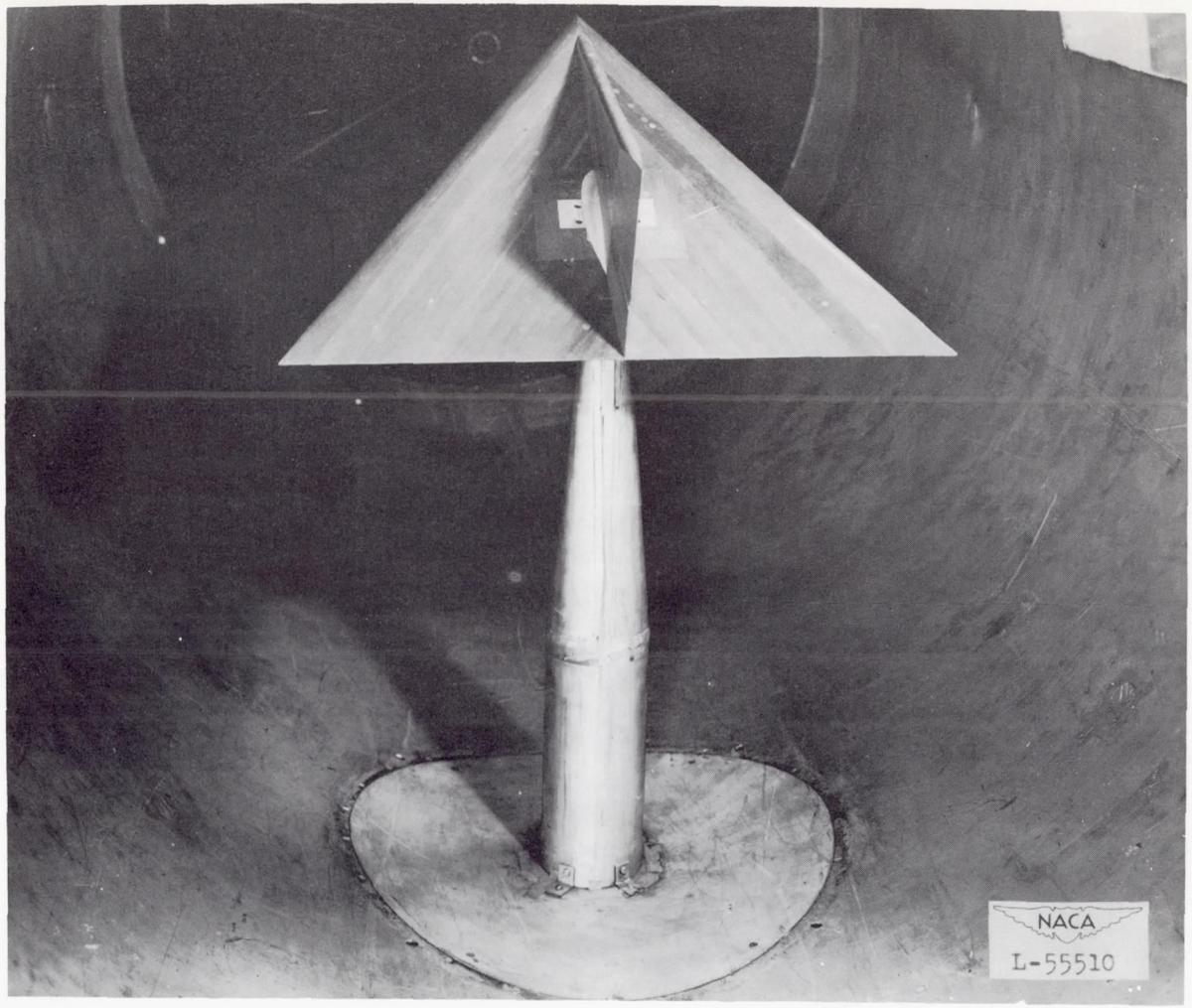

Figure 5.– Model 5 mounted in tunnel. A_{wing} = 2.31; A_{fin} = 0.77. Profile of wing, NACA 0012; profile of fin, flat plate.

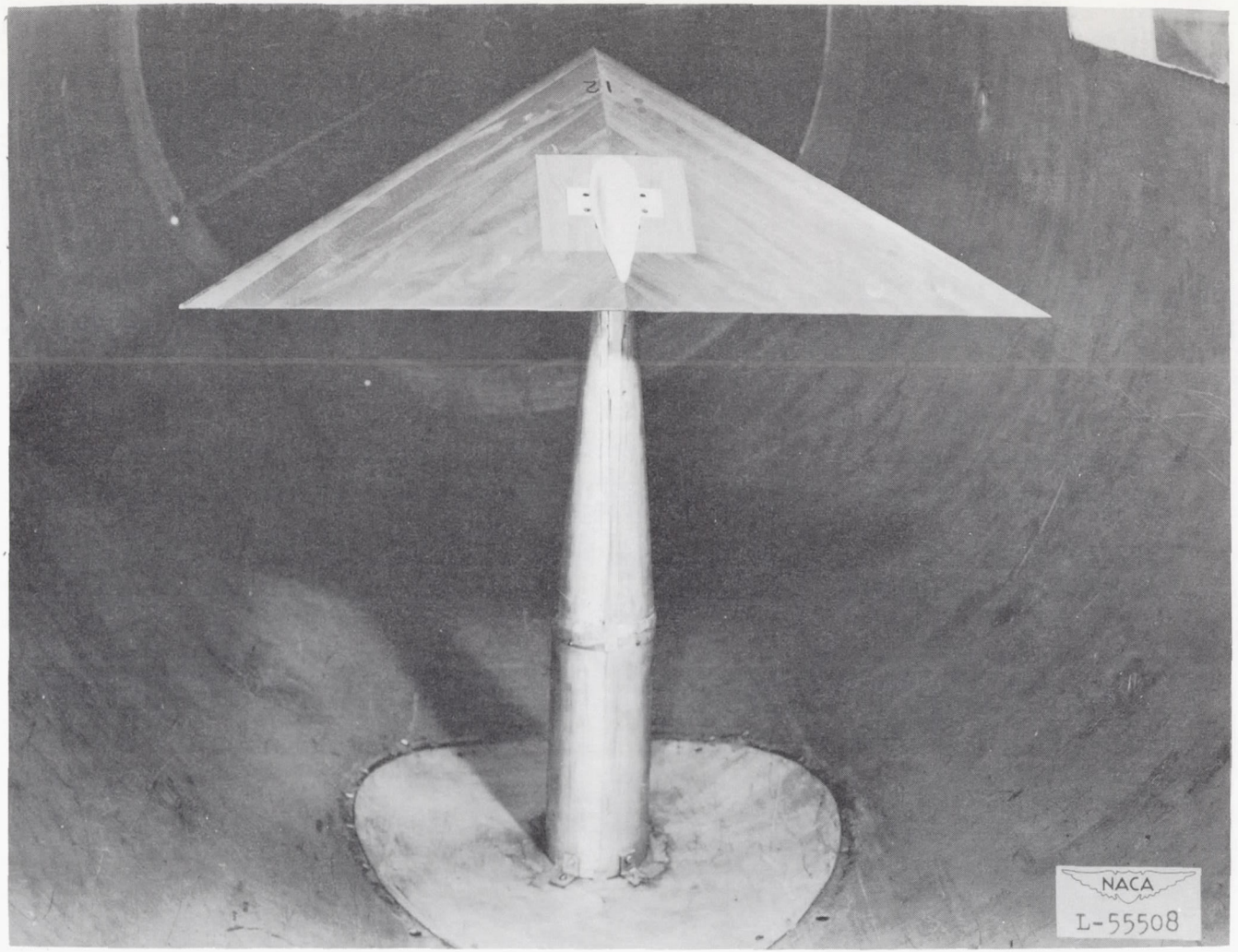

Figure 6.– Model 7 mounted in tunnel. $A = 4$; $\Lambda_{c/4} = 36.9^{\circ}$; profile, NACA 0012.

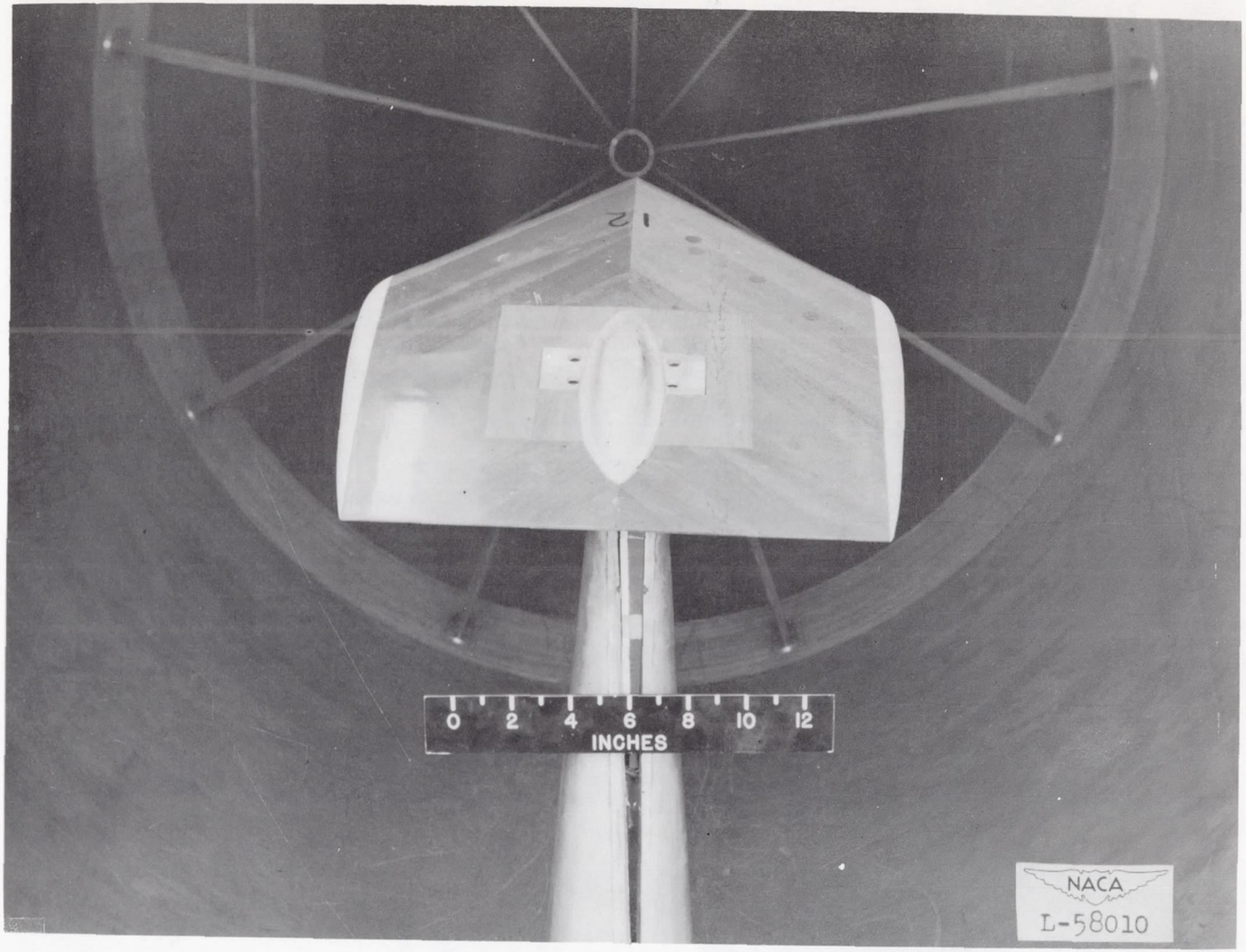

Figure 7.— Model 10 mounted in tunnel. $A = 1.0$; $\Lambda_{c/4} = 36.9^{\circ}$; $\lambda = 0.58$. Profile, NACA 0012.

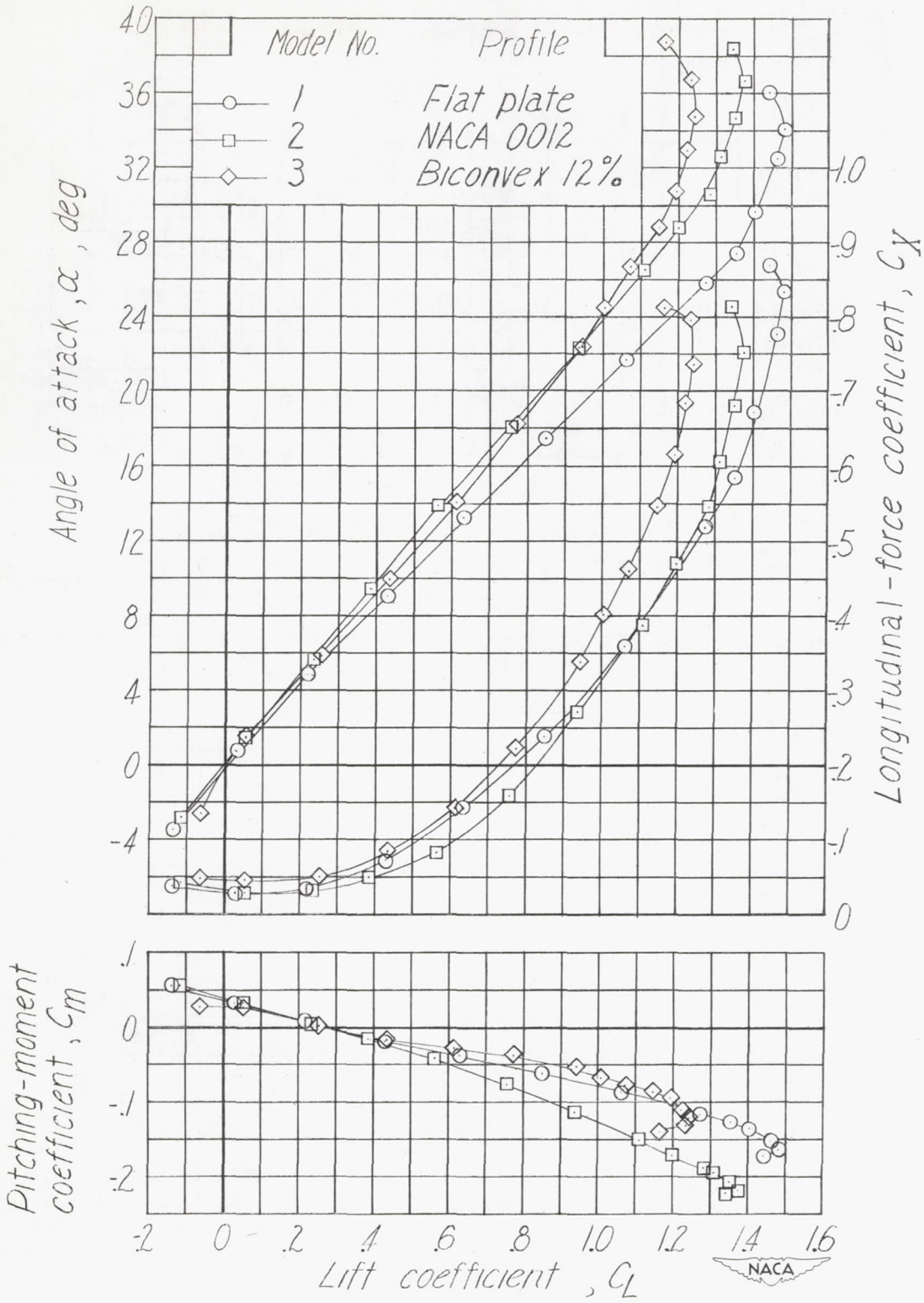

Figure 8.– Effect of profile on aerodynamic characteristics of a triangular wing of aspect ratio 2.31. $\Lambda_{c/4} = 52.2^{\circ}$.

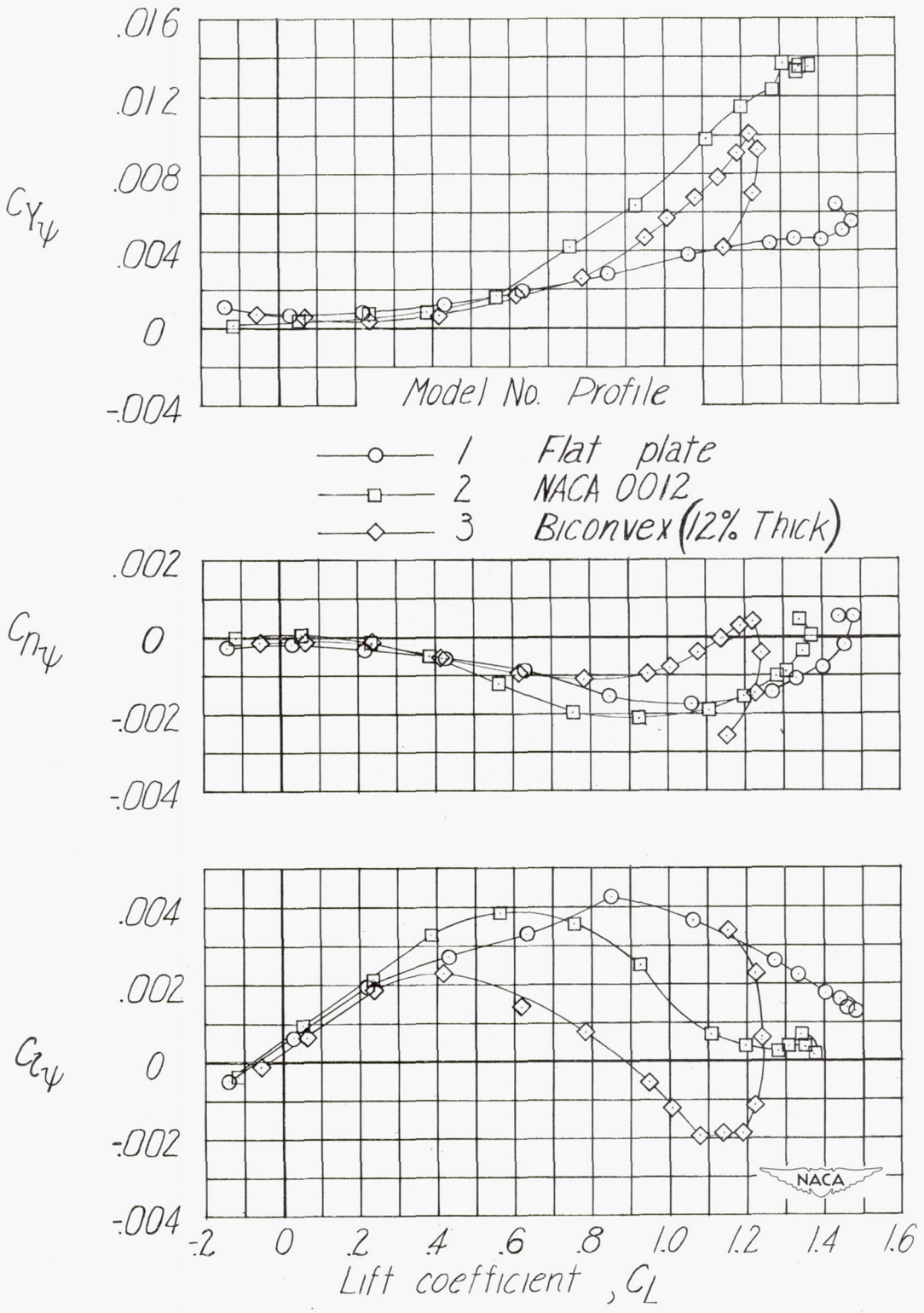

Figure 9.– Effect of profile of a triangular wing of aspect ratio 2.31 on C_{Y_ψ}, C_{n_ψ}, and C_{l_ψ}. $\Lambda_{c/4} = 52.2^\circ$.

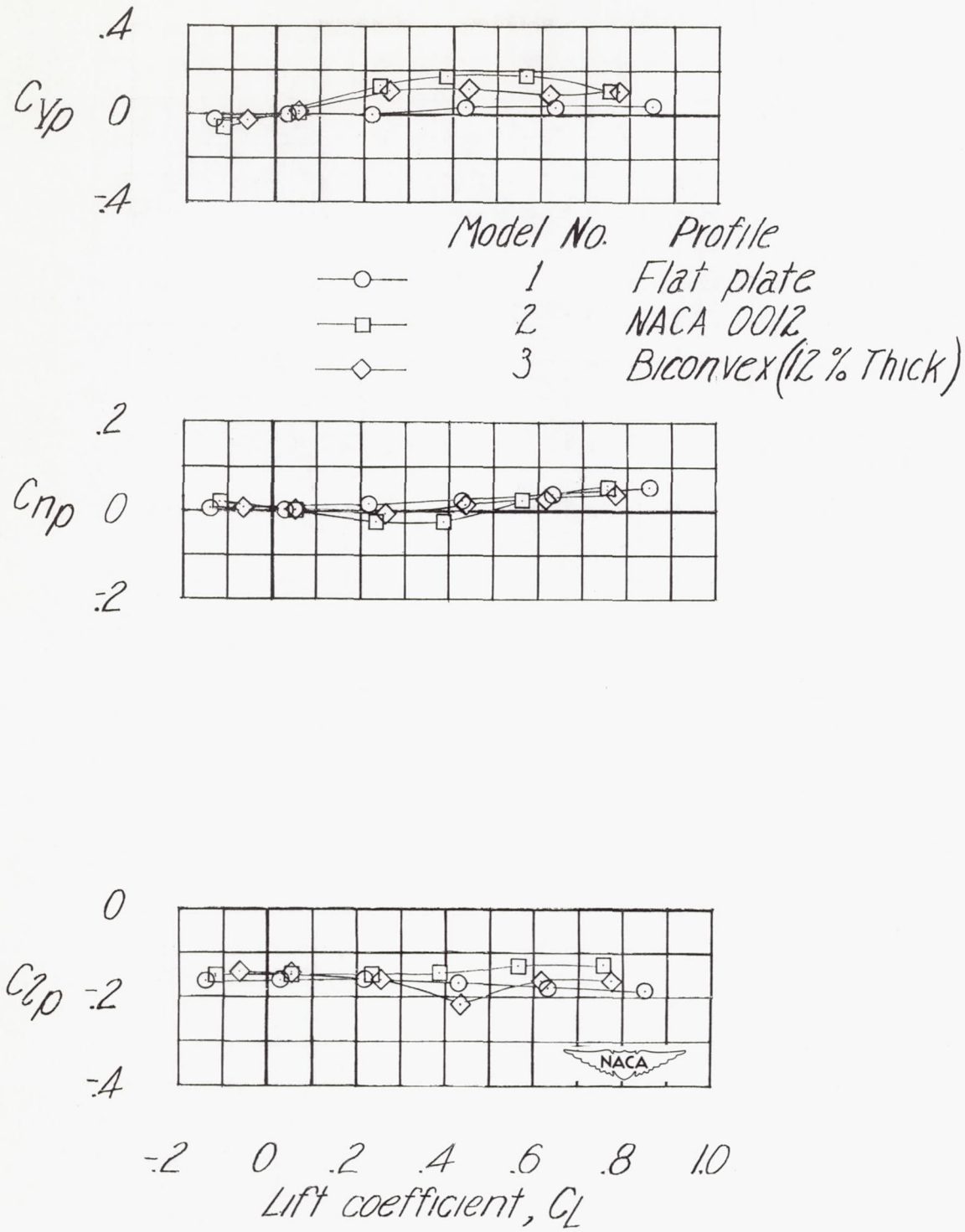

Figure 10.– Effect of profile of a triangular wing of aspect ratio 2.31 on C_{Y_p}, C_{n_p}, and C_{l_p}. $\Lambda_c/4 = 52.2^\circ$.

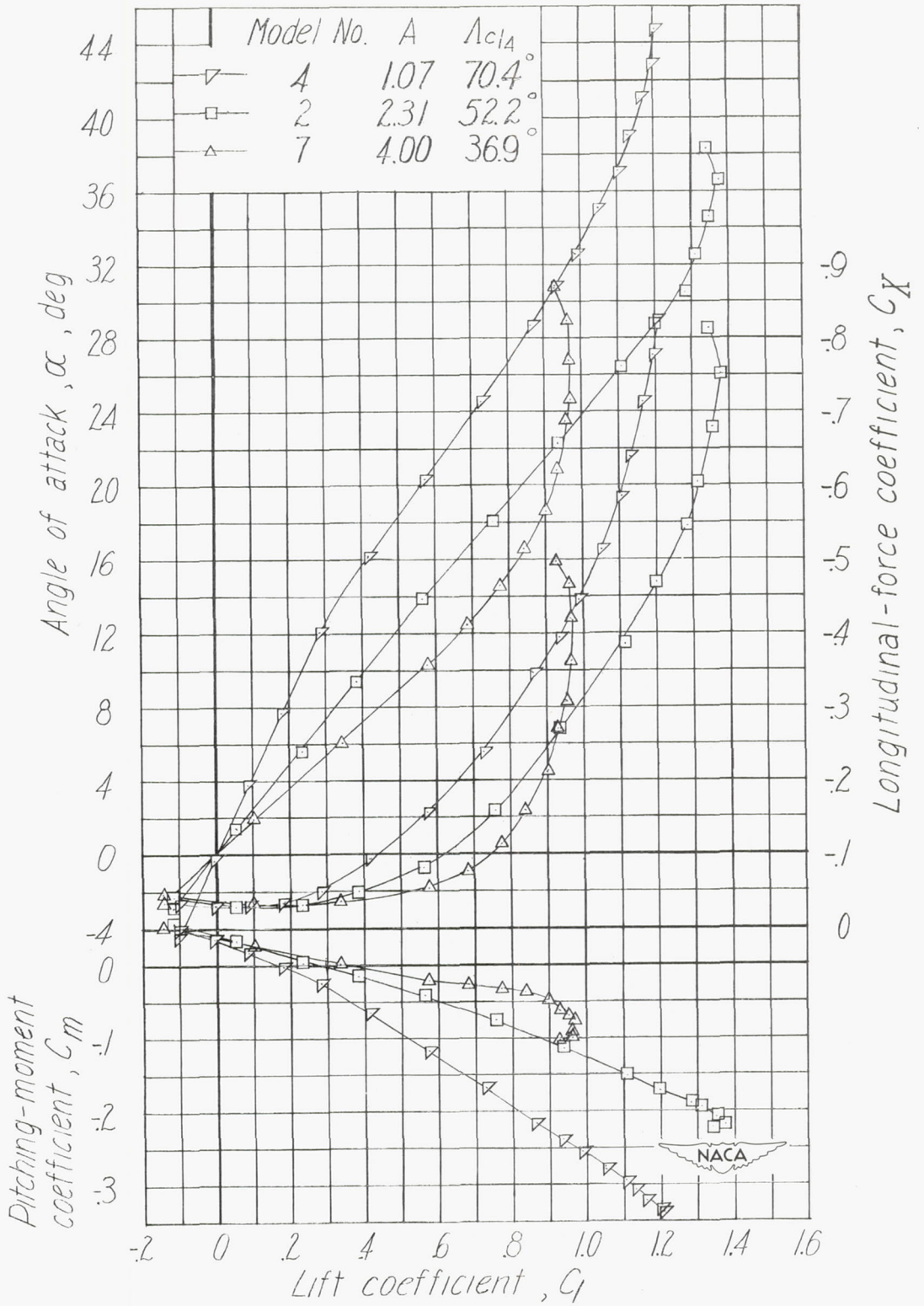

Figure 11.– Effect of aspect ratio on aerodynamic characteristics of triangular wings of NACA 0012 profile.

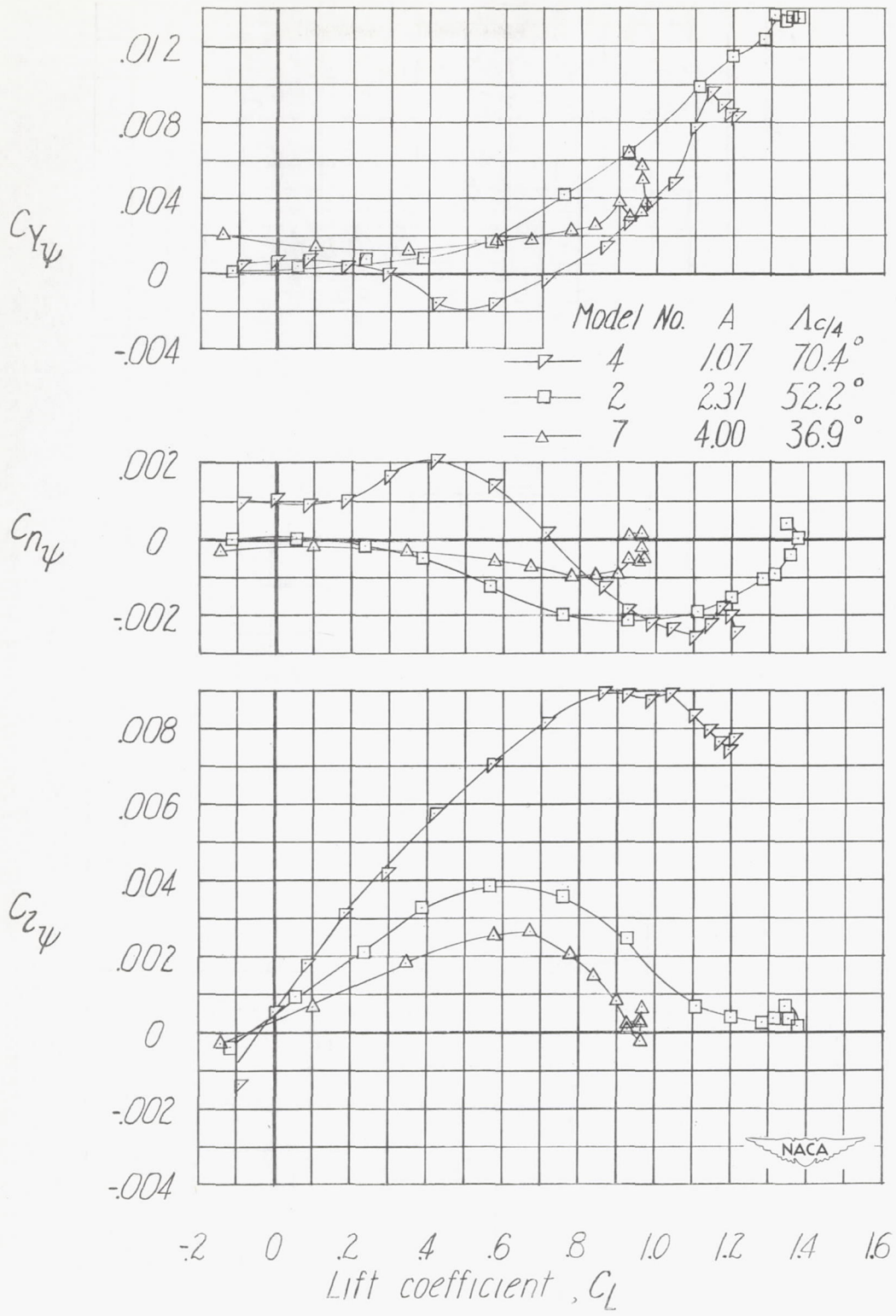

Figure 12.– Effect of aspect ratio of triangular wings of NACA 0012 profile on C_{Y_ψ}, C_{n_ψ}, and C_{l_ψ}.

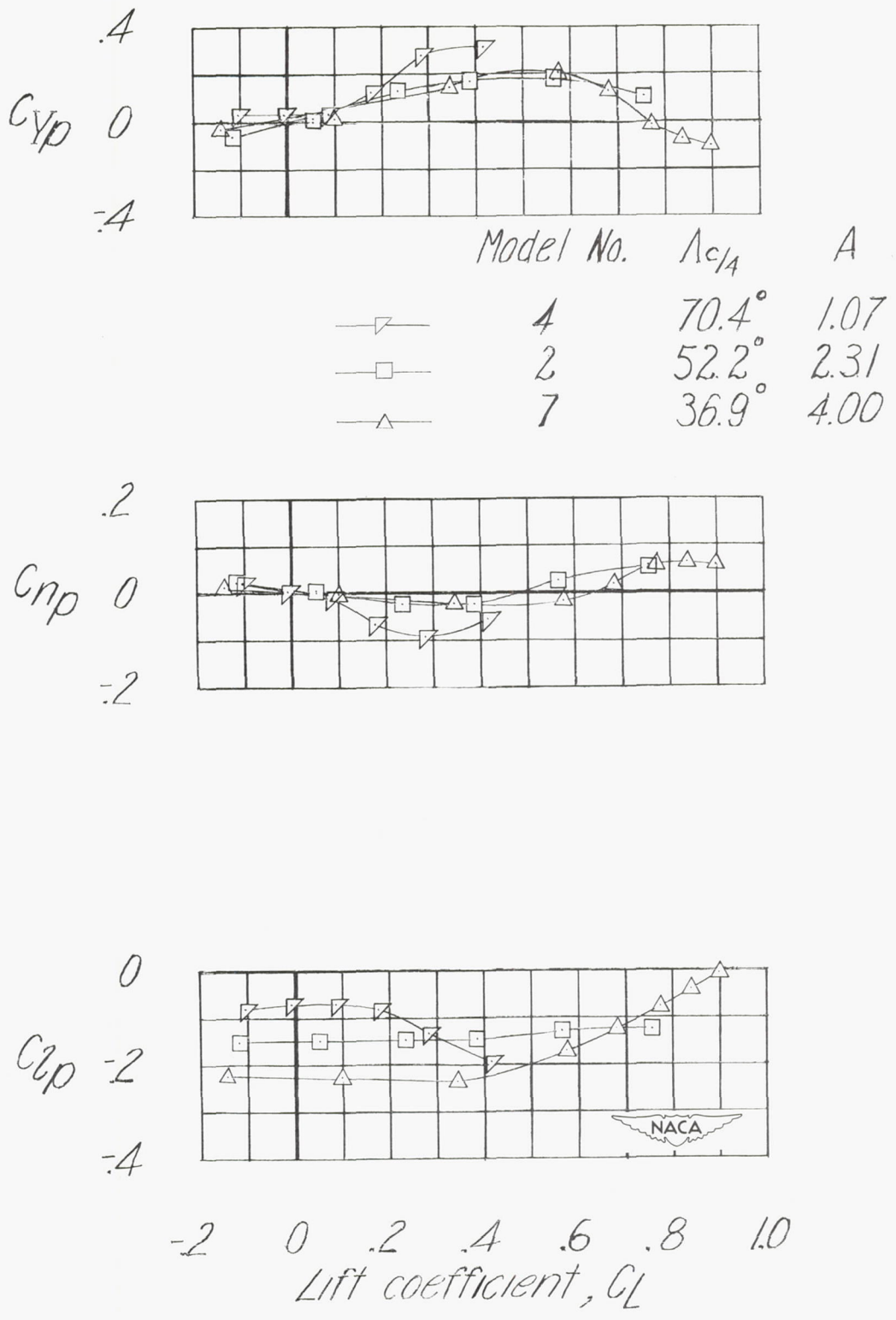

Figure 13.– Effect of aspect ratio of triangular wings of NACA 0012 profile on C_{Y_p}, C_{n_p}, and C_{l_p}.

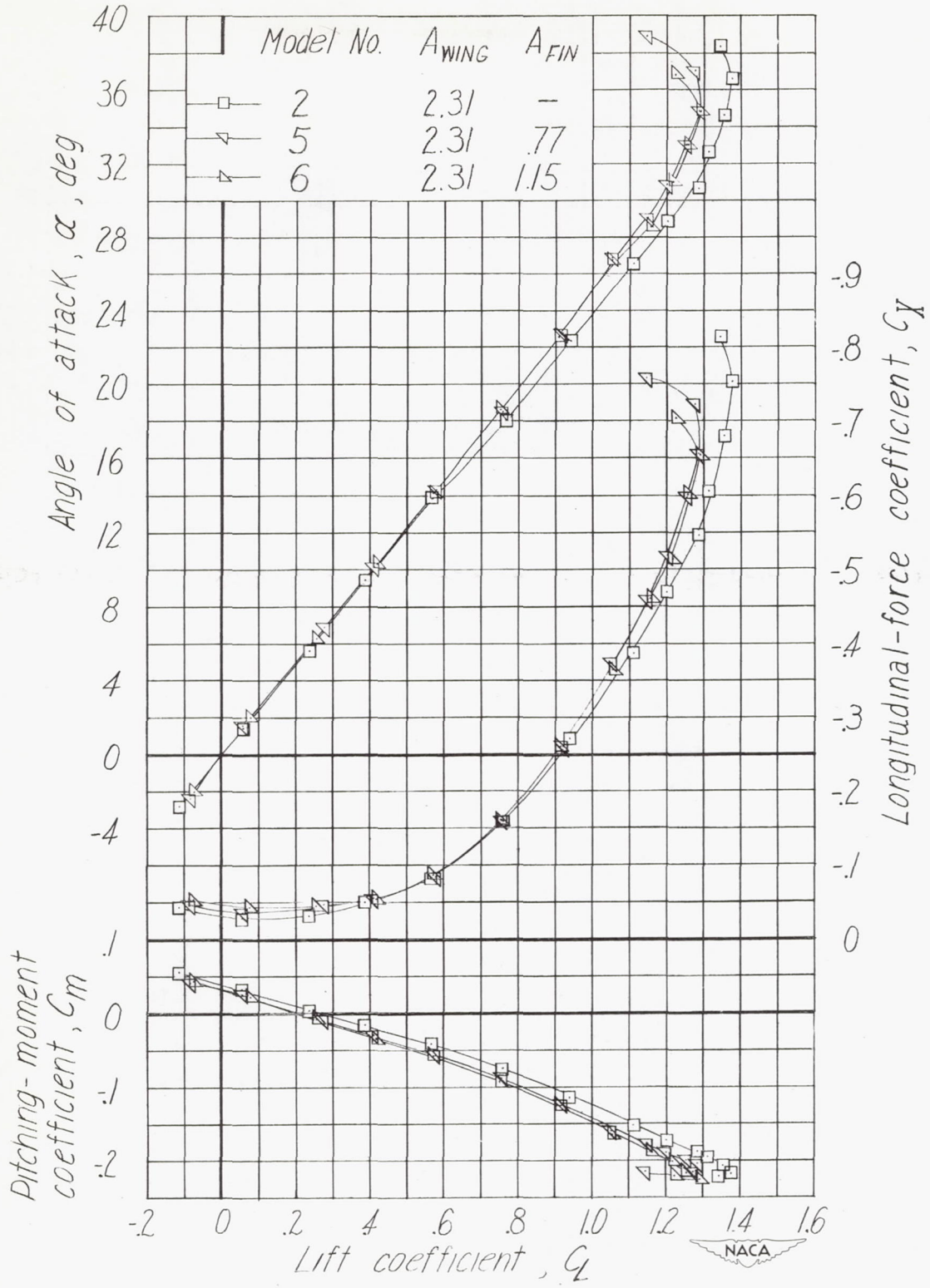

Figure 14.— Effect of fins on aerodynamic characteristics of a triangular wing of NACA 0012 profile. $\Lambda_{c/4} = 52.2^{\circ}$.

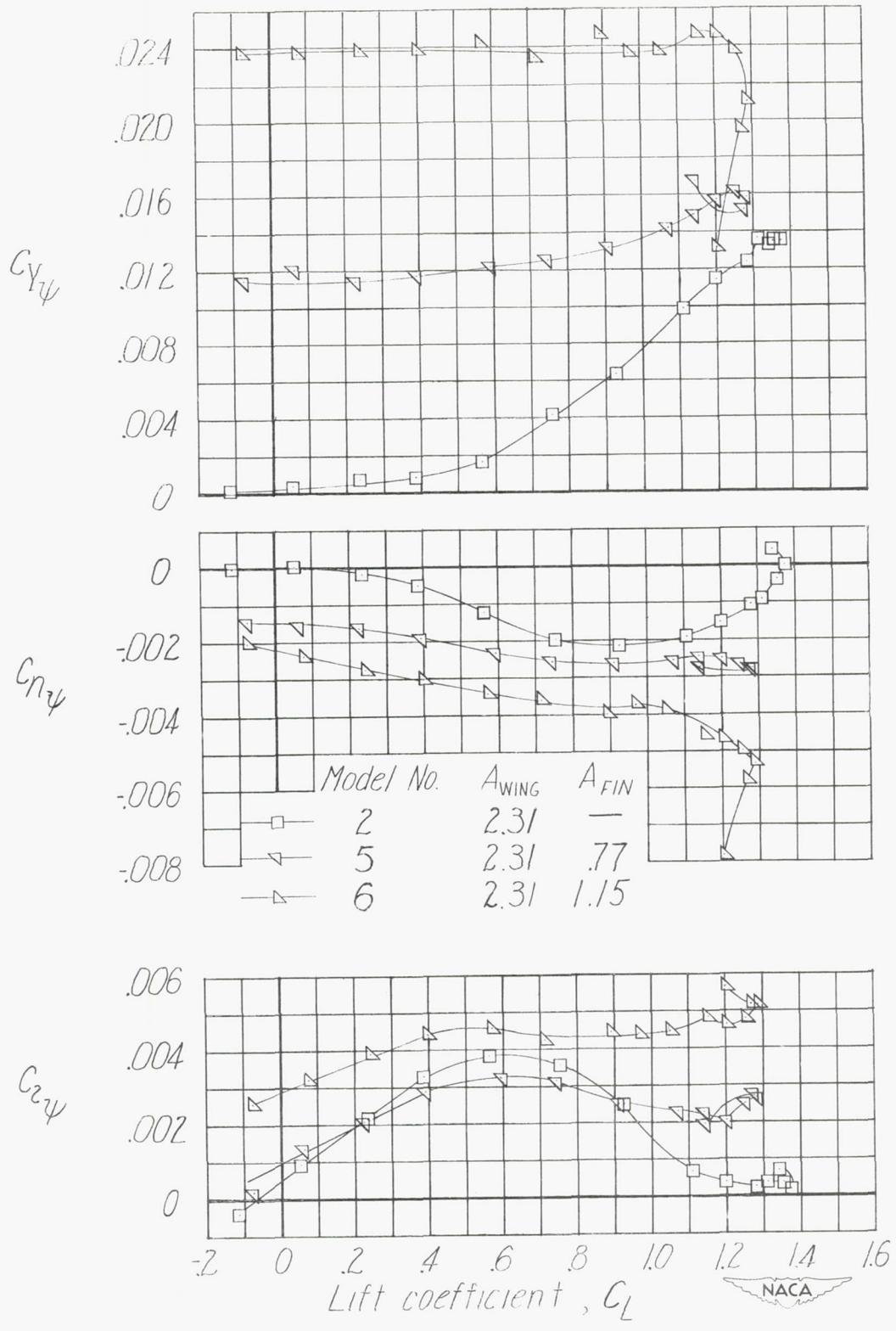

Figure 15.— Effect of fins on a triangular wing of NACA 0012 profile on C_{Y_ψ}, C_{n_ψ}, and C_{l_ψ}. $\Lambda_{c/4} = 52.2^\circ$.

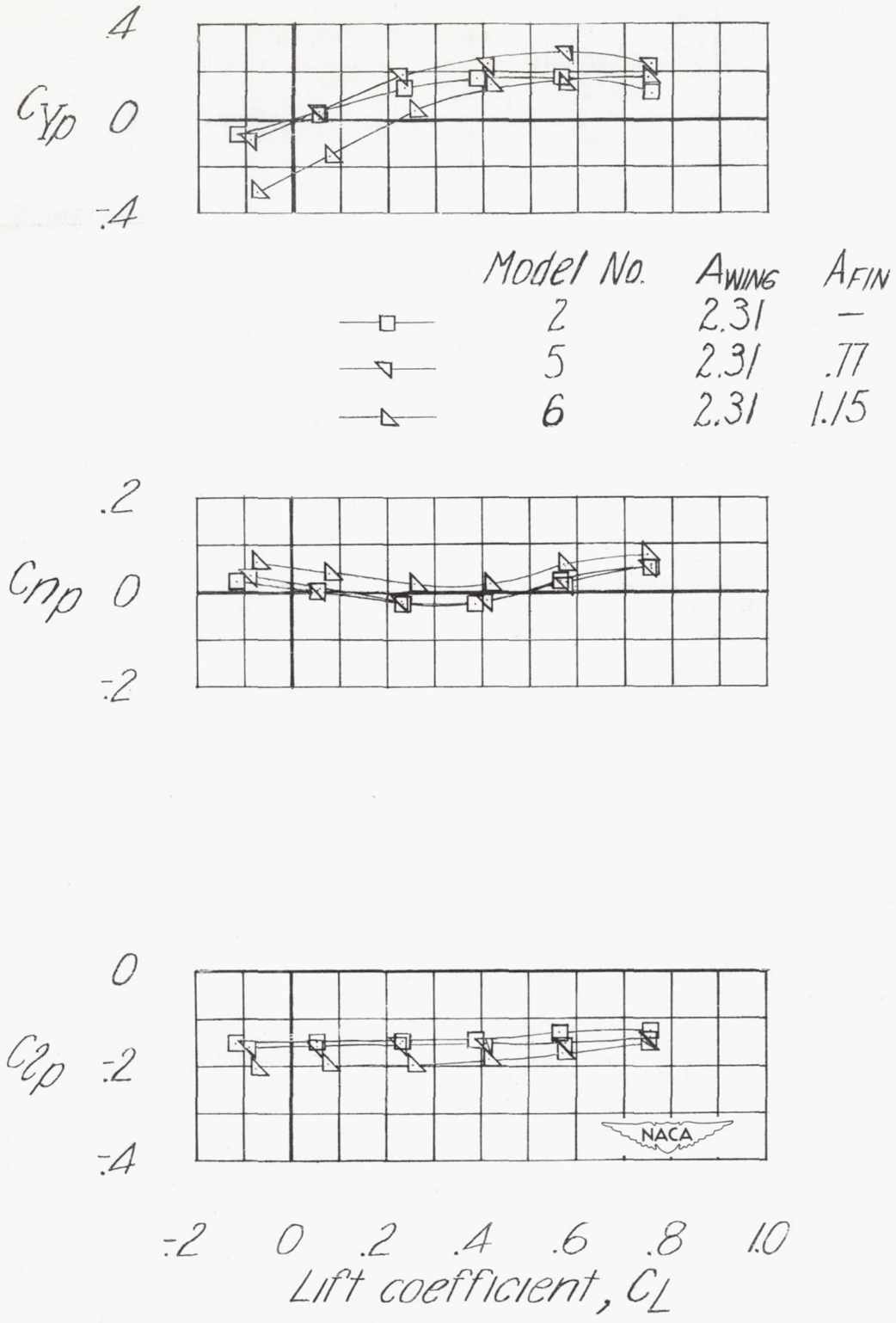

Figure 16.– Effect of fins on a triangular wing of NACA 0012 profile on C_{Y_p}, C_{n_p}, and C_{l_p}. $\Lambda_c/4 = 52.2^\circ$.

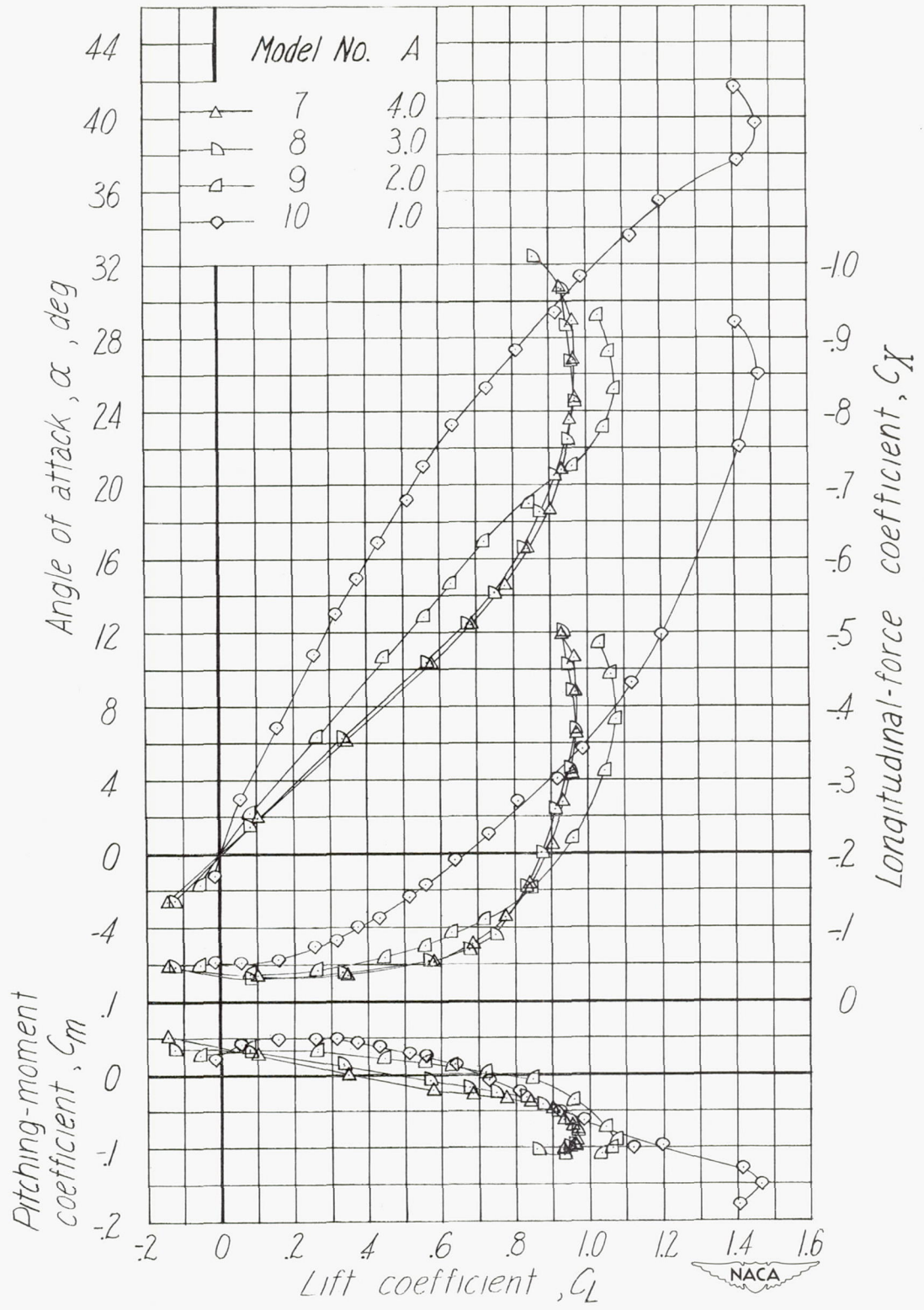

Figure 17.– Effect of aspect ratio on aerodynamic characteristics of modified triangular wings. $\Lambda_{c/4} = 36.9^{\circ}$.

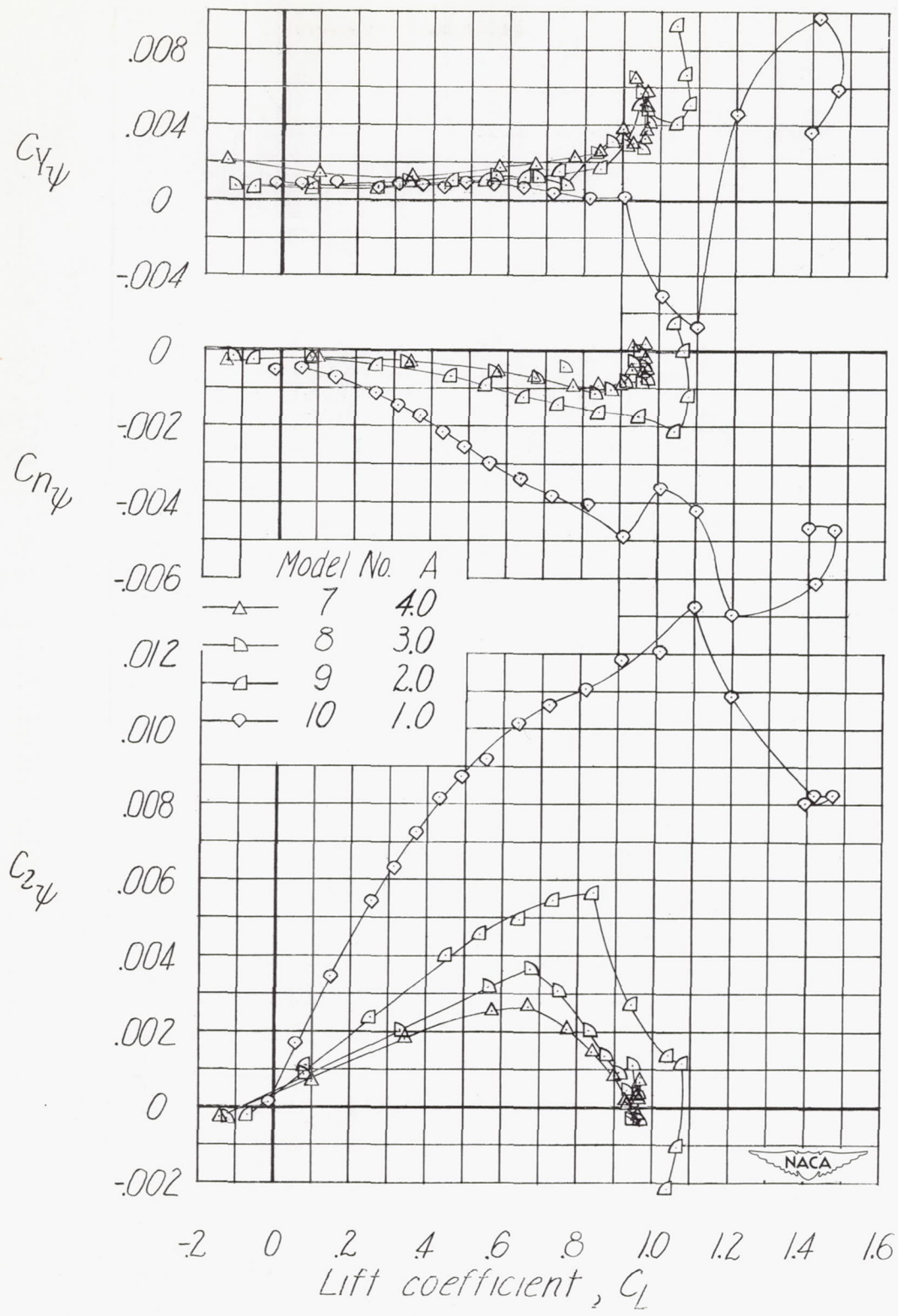

Figure 18.- Effect of aspect ratio of modified triangular wings of NACA 0012 profile on C_{Y_ψ}, C_{n_ψ}, and C_{l_ψ}. $\Lambda_{c/4} = 36.9^\circ$.

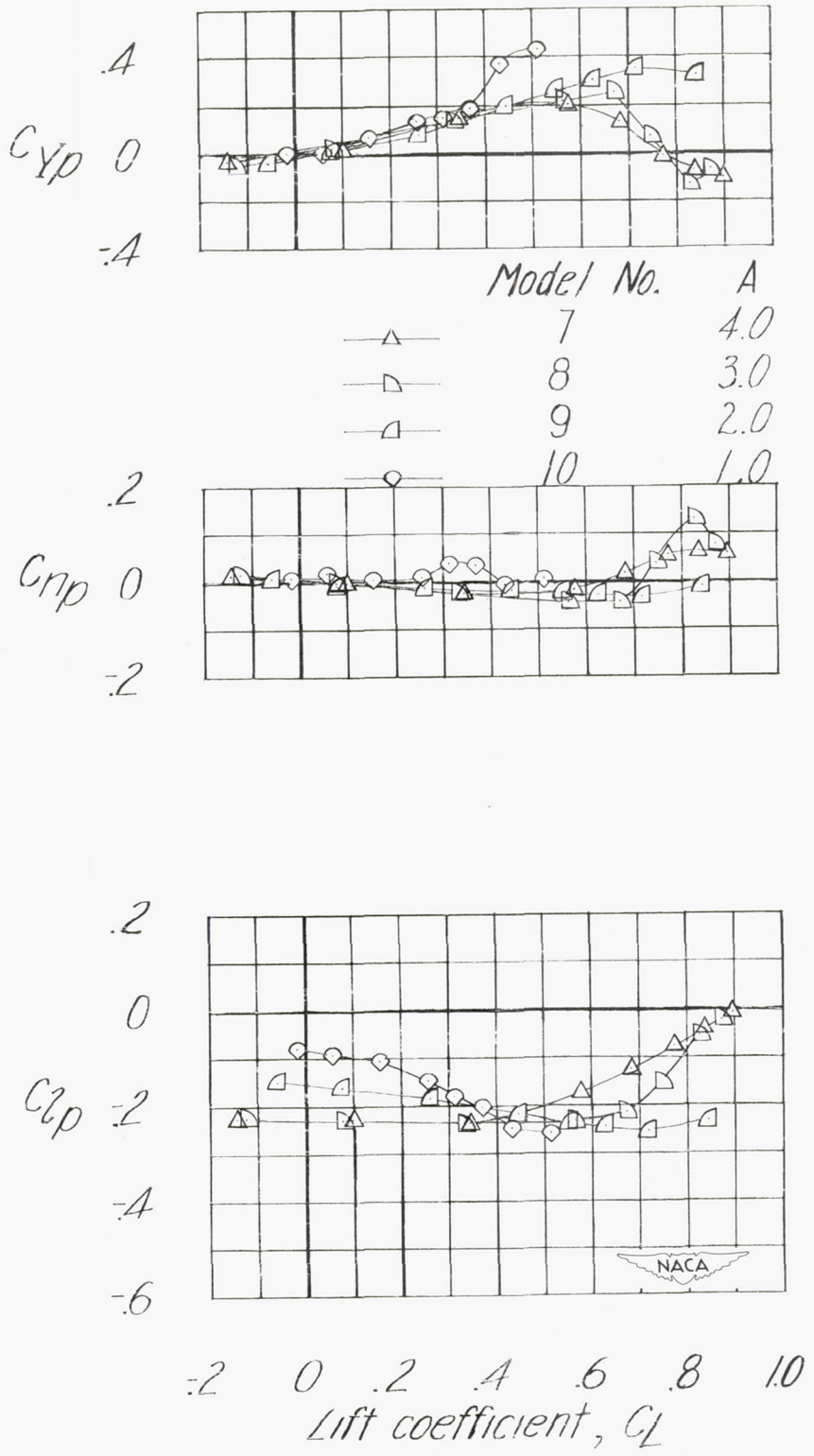

Figure 19.– Effect of aspect ratio of modified triangular wings of NACA 0012 profile on C_{Y_p}, C_{n_p}, and C_{l_p}. $\Lambda_{c/4} = 36.9^\circ$.

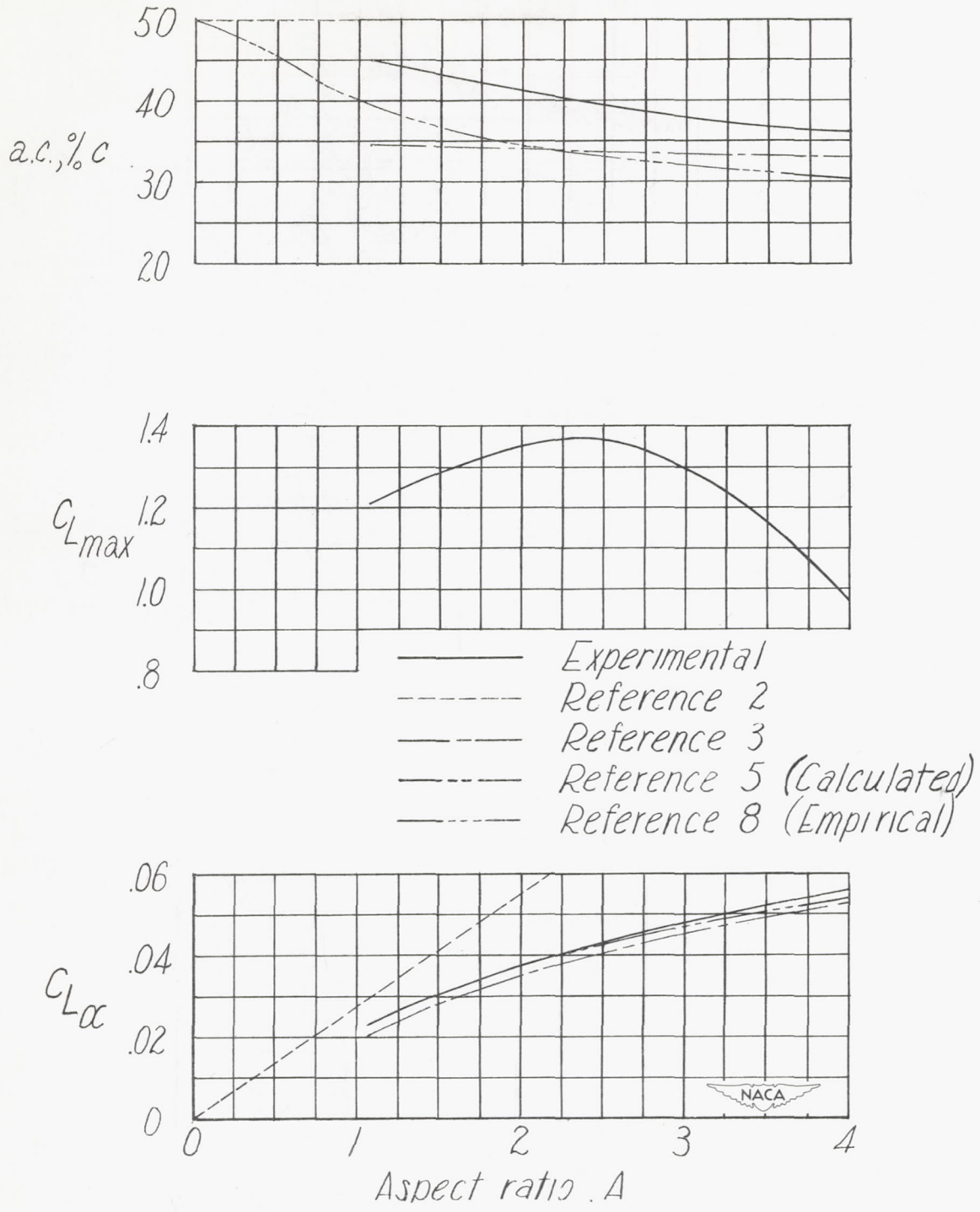

Figure 20.– Variation of aerodynamic center $C_{L_{max}}$ and C_{L_α} with aspect ratio for wings of triangular plan form. Profile, NACA 0012; $C_L = 0$.

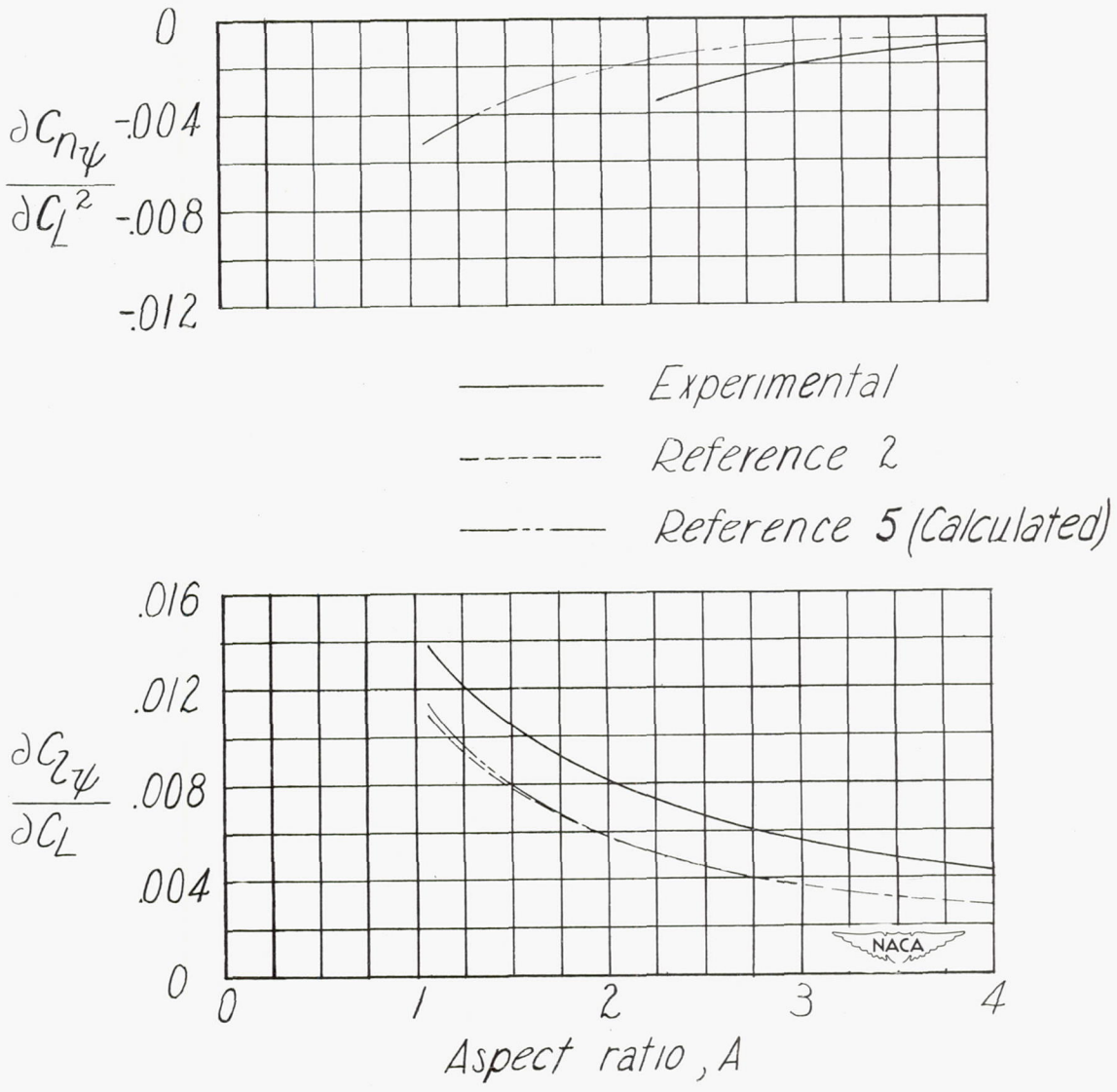

Figure 21.– Variation of $\partial C_{n_\psi}/\partial C_L^2$ and $\partial C_{l_\psi}/\partial C_L$ with aspect ratio for wings of triangular plan form. Profile, NACA 0012; $C_L = 0$.

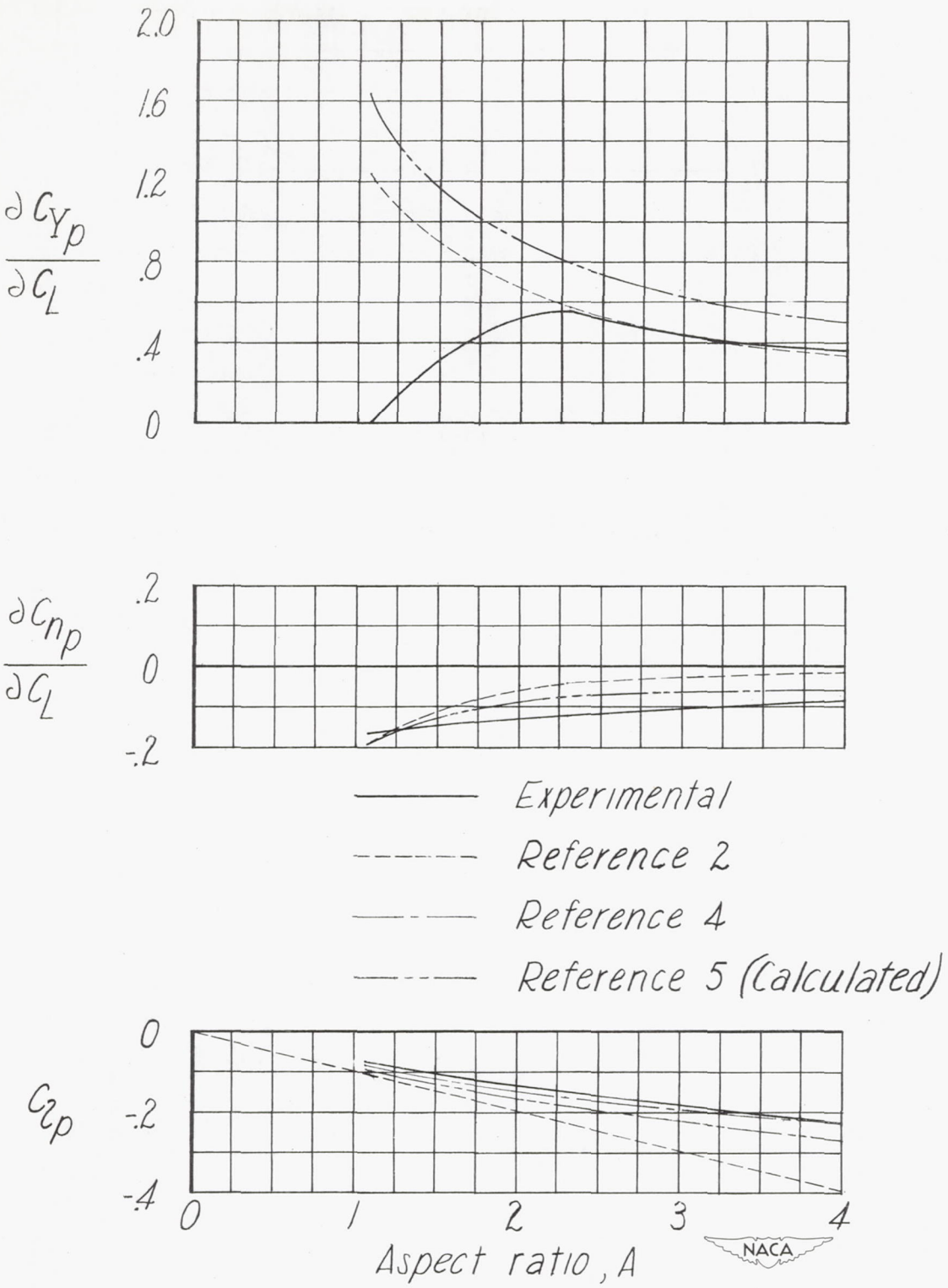

Figure 22.– Variation of $\partial C_{Y_p}/\partial C_L$, $\partial C_{n_p}/\partial C_L$, and C_{l_p} with aspect ratio for wings of triangular plan form. Profile, NACA 0012; $C_L = 0$.

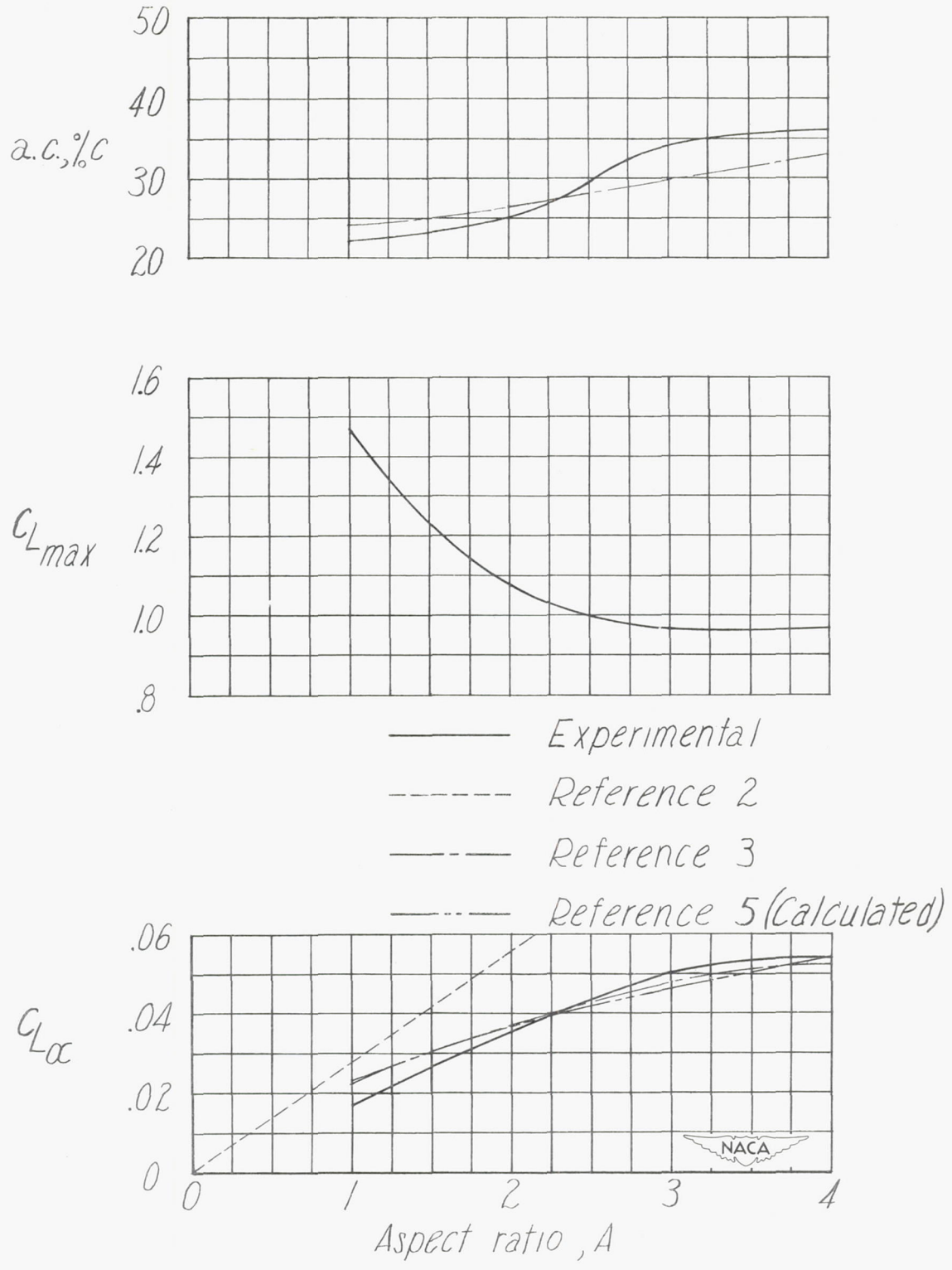

Figure 23.– Variation of aerodynamic center, $C_{L_{max}}$, and C_{L_α} with aspect ratio for modified triangular wings. Profile, NACA 0012; $\Lambda_{c/4} = 36.9^\circ$; $C_L = 0$.

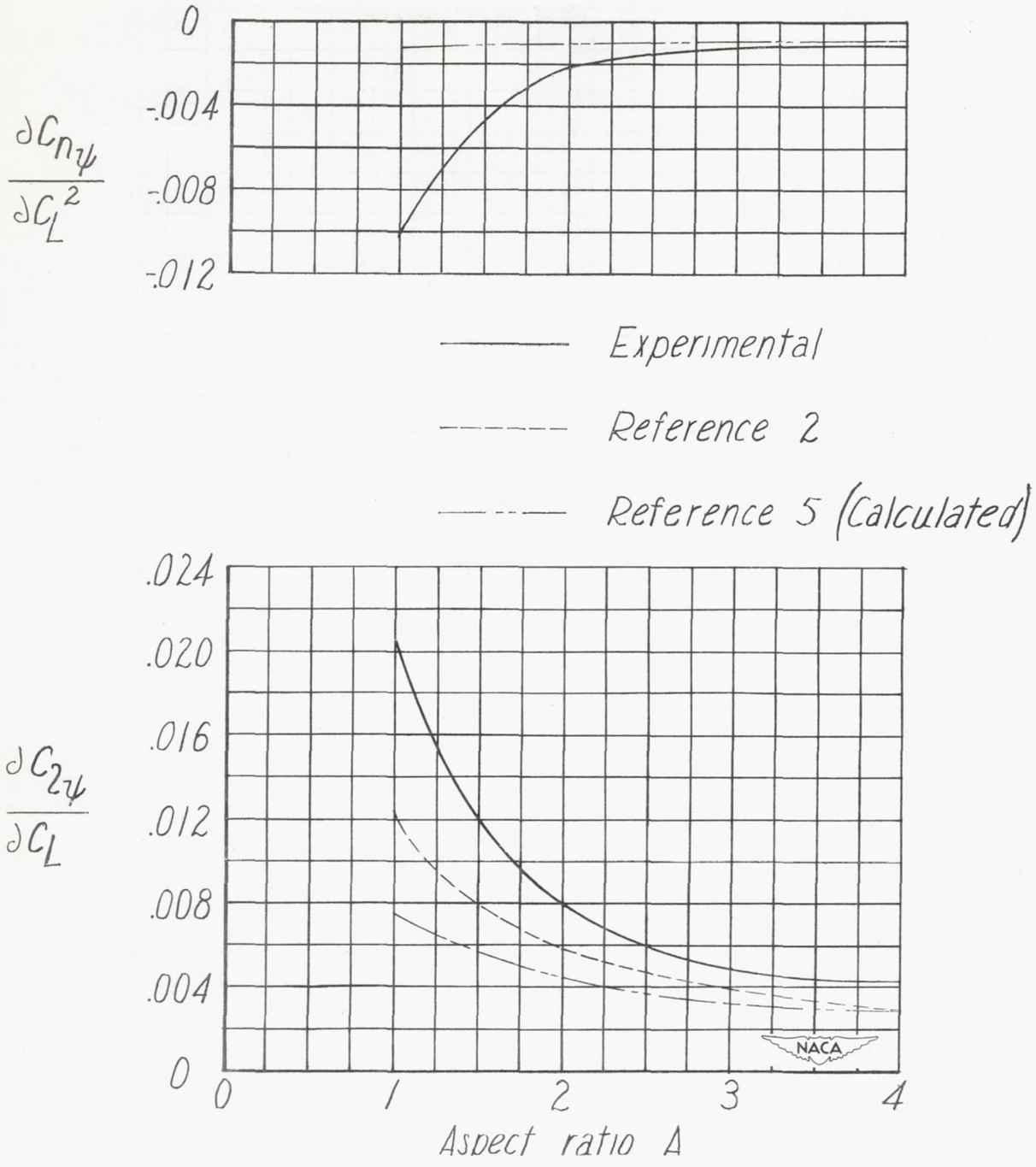

Figure 24.- Variation of $\partial C_{n_\psi}/\partial C_L{}^2$ and $\partial C_{l_\psi}/\partial C_L$ with aspect ratio for modified triangular wings. Profile, NACA 0012; $\Lambda_{c/4} = 36.9°$; $C_L = 0$.

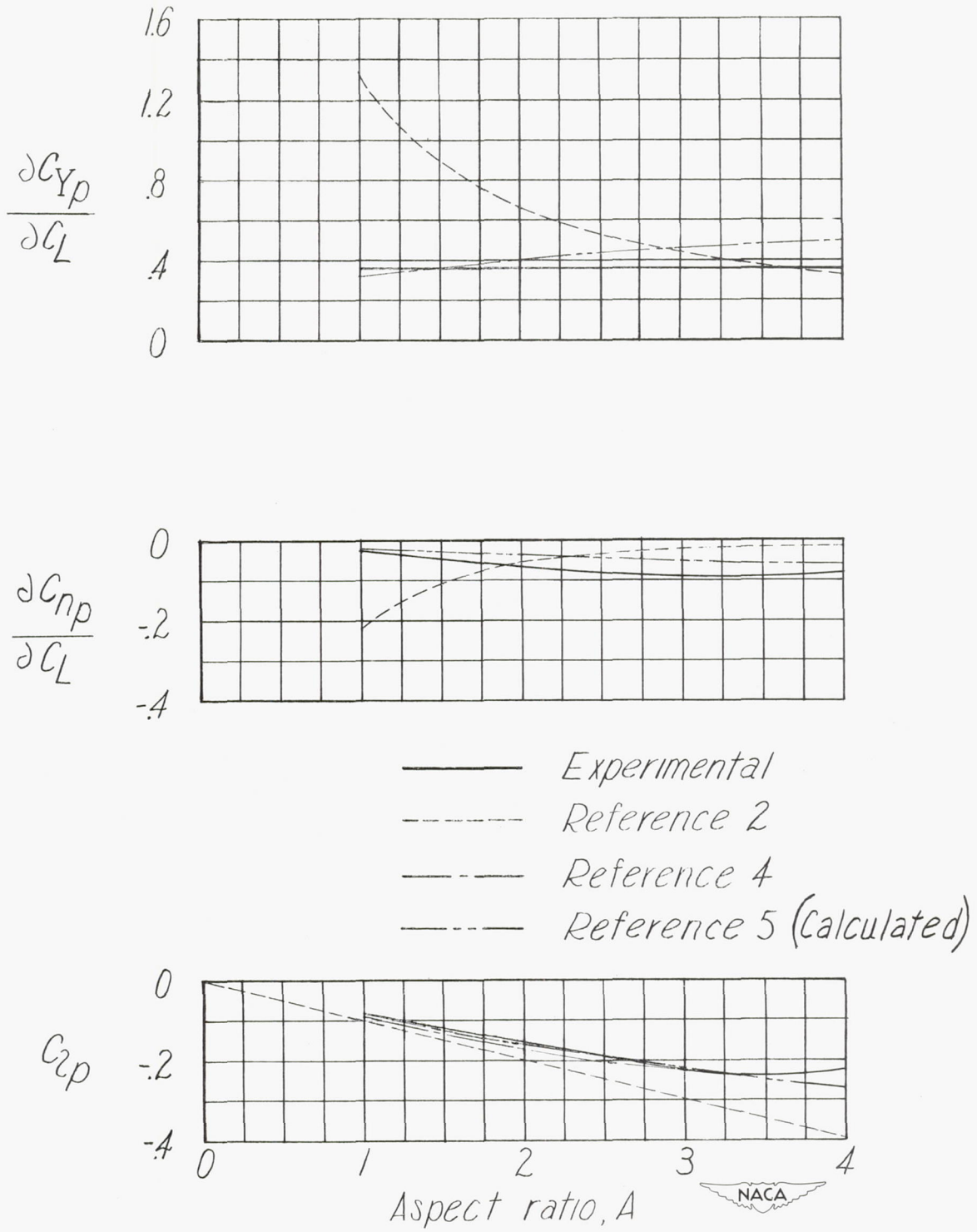

Figure 25.– Variation of $\partial C_{Y_p}/\partial C_L$, $\partial C_{n_p}/\partial C_L$, and C_{l_p} with aspect ratio for modified triangular wings. Profile, NACA 0012; $\Lambda_{c/4} = 36.9^\circ$; $C_L = 0$.